**Earth Surface Processes and Landforms**
*Earth Surf. Process. Landforms* **32**, 1947–1970 (2007)
Published online 11 April 2007 in Wiley InterScience
(www.interscience.wiley.com) **DOI:** 10.1002/esp.1508

# Persistence of road runoff generation in a logged catchment in Peninsular Malaysia

Alan D. Ziegler,[1]* Junjiro N. Negishi,[2] Roy C. Sidle,[3] Takashi Gomi,[3] Shoji Noguchi[4] and Abdul Rahim Nik[5]

[1] *Geography Department, University of Hawaii, Honolulu HI, USA*
[2] *Aqua Restoration Research Center, Public Works Research Institute, Kawashima, Kakamigahara, Gifu, Japan*
[3] *Disaster Prevention Research Institute, Geohazards Division, Kyoto University, Kyoto, Japan*
[4] *Forestry and Forest Product Research Institute, Tohoku Research Center, Japan*
[5] *Forest Research Institute Malaysia, Kuala Lumpur, Malaysia*

**Correspondence to: A. D. Ziegler, Department of Geography, 2424 Maile Way, 445 Saunders Hall, University of Hawaii at Manoa, Honolulu, HI 96822, USA.
E-mail: adz@hawaii.edu*

## Abstract

**Measurements of saturated hydraulic conductivity ($K_s$) and diagnostic model simulations show that all types of logging road/trail in the 14·4 ha Bukit Tarek Experimental Catchment 3 (BTEC3) generate substantial Horton overland flow (HOF) during most storms, regardless of design and level of trafficking. Near-surface $K_s$(0–0·05 m) on the main logging road, skid trails and newly constructed logging terraces was less than 1, 2 and 34 mm h$^{-1}$, respectively. Near-surface $K_s$ on an abandoned skid trail in an adjacent basin was higher (62 mm h$^{-1}$), owing to the development of a thin organic-rich layer on the running surface over the past 40 years. Saturated hydraulic conductivity measured at 0·25 m below the surface of all roads was not different (all <6 mm h$^{-1}$) and corresponded to the $K_s$ of the adjacent hillslope subsoil, as most roads were excavated into the regolith more than 0·5–1 m. After 40 years, only limited recovery in near-surface $K_s$ occurred on the abandoned skid trail. This road generated HOF after the storage capacity of the upper near-surface layer was exceeded during events larger than about 20 mm. Thus, excavation into low-$K_s$ substrate had a greater influence on the persistence of surface runoff production than did surface compaction by machinery during construction and subsequent use during logging operations. Overland flow on BTEC3 roads was also augmented by the interception of shallow subsurface flow traveling along the soil–saprolite/bedrock interface and return flow emerging from the cutbank through shallow biogenic pipes. The most feasible strategy for reducing long-term road-related impacts in BTEC3 is limiting the depth of excavation and designing a more efficient road network, including minimizing the length and connectivity of roads and skid trails. Copyright © 2007 John Wiley & Sons, Ltd.**

**Keywords: bulk density; Horton overland flow (HOF); interception of subsurface storm flow (ISSF); logging impact recovery; runoff generation; saturated hydraulic conductivity ($K_s$)**

Received 1 July 2006;
Revised 23 January 2007;
Accepted 7 February 2007

## Introduction

Logging roads play a key role in water quality degradation, disruption of stream ecological processes and sedimentation in downstream water systems and impoundments (see, e.g., Hafley, 1975; Cederholm *et al.*, 1981; Megahan, 1988; Fahey and Coker, 1992; Grayson *et al.*, 1993; MacDonald *et al.*, 2001; Forman and Alexander, 1998; Jones *et al.*, 2000; Lane and Sheridan, 2002; Sidle *et al.*, 2006). Various hydrologic impacts of logging roads are now recognized (Bruijnzeel, 1990; Gucinski *et al.*, 2000; Sidle and Ochiai, 2006). For example, roads and skid trails have a high propensity for generating runoff by the Hortonian overland flow mechanism (HOF) and by intercepting subsurface flow (ISSF) at the cutbank (Megahan, 1972; Burroughs *et al.*, 1972; Van der Plas and Bruijnzeel, 1993; Ziegler and Giambelluca, 1997). Because roads can affect the efficiency with which hillslope water is delivered to the stream system (Wemple *et al.*, 1996), they potentially alter stormflow hydrographs. The extent to which such alterations occur remains in question, as noted in both field and modeling studies during the last few decades (cf. Reinhart, 1964; Harr *et al.*, 1975; Ziemer, 1981; Megahan, 1983; King and Tennyson, 1984; Bren and Leitch, 1985; Keppeler and Ziemer, 1990; Storck *et al.*, 1997; Thomas and Megahan, 1998; Jones, 2000; La Marche and Lettenmaier, 2001; Guillemette *et al.*, 2005).

An inherent linkage exists between the alteration of stormflow pathways by roads and road-related geomorphological impacts. For example, concentrated road runoff is not only a principal agent of erosion and sediment production on unpaved surfaces, but when diverted onto adjacent hillslopes it may initiate gully erosion, channel headcutting and mass wasting, especially in poorly consolidated fill materials (Swift, 1984; Reid and Dunne, 1984; Montgomery, 1994; Luce and Black, 1999; Jones *et al.*, 2000; Ziegler *et al.*, 2000; MacDonald *et al.*, 2001; Wemple *et al.*, 2001; Croke *et al.*, 2006; Sidle and Ochiai, 2006). The extent to which roads affect catchment geomorphic processes is related in part to the total extent of the road network, degree of traffic, type of excavation (e.g. scraping versus deep excavation), road location and connectivity of the road network with the stream channel.

Few studies provide direct insight regarding the amount of time hydro-geomorphological processes will be disrupted following initial road building. In one study, Megahan (1974) reported that, while most of the accelerated surface erosion on roads in Idaho (USA) occurred in the first year following building, elevated rates could persist for decades (cf. Beschta, 1978). Sidle *et al.* (2004) reported that nearly 80% of the soil loss from a logging road system in a managed forest in Peninsular Malaysia was delivered to the stream in the first 16 months. Other works suggest sediment generation from the road prism persists even after abandonment because unstable cutbanks and fillslopes are prone to failure, particularly during large storms (Douglas *et al.*, 1999; Wemple *et al.*, 2001; Chappell *et al.*, 2004).

Surface compaction studies provide indirect evidence that roads/tracks can accelerate HOF generation for several decades following abandonment (Dickerson, 1976; Froehlich, 1979; Greacen and Sands, 1980; Jakobsen, 1983; Incerti *et al.*, 1987; Croke *et al.*, 2001; Rab, 2004; Webb, 2002). Kamaruzaman (1996) estimated 50 years was needed for the recovery of saturated hydraulic conductivity ($K_s$) on skid trails in Peninsular Malaysia. Perry (1964) noted that 40 years was a conservative estimate of the amount of time for infiltration to recover on abandoned logging roads at a Southeast USA site; he further indicated that recovery time was site specific.

Clearly, more research is needed to advance our understanding of the long-term impacts of roads, and the appropriate means for rehabilitation (Luce, 2002; Allison *et al.*, 2004). Herein, we address this issue through field measurements of $K_s$ and simulations of HOF on several types of logging road at the Bukit Tarek Experimental Catchments (BTEC) research site in Peninsular Malaysia. In particular, we investigate two questions: (1) how does hydrological response vary among roads differing in manner of construction and usage and (2) what effect does natural vegetation recovery have on hydrological response on abandoned skid trails?

## Study Area

### Bukit Tarek Experimental Catchment

The study was conducted in catchment 3 (BTEC 3) of the Bukit Tarek Experimental Watershed site located within compartment 41 of Bukit Tarek Tambahan Forest Reserve in Selangor Darul Ehsan, approximately 60 km NW of Kuala Lumpur, Peninsular Malaysia (3° 31′ 30″ N, 101° 35′ E) (Saifuddin *et al.*, 1991) (Figure 1(b)). The catchment area is 14·4 ha; the length of the main channel is 340 m and the length of perennial tributary streams is 145 m (Gomi *et al.*, 2006). Additional ephemeral tributary streams increase the total length of the channel network to about 650 m. Elevation ranges from 40 to 140 m asl. Annual rainfall is approximately 2400 mm (Noguchi *et al.*, 1996), falling during two principal monsoon seasons: April–May and October–November. The average annual rain day total is 150 days (Saifuddin *et al.*, 1991). During the period 1992–1994, Noguchi *et al.* (1996) found that November was the wettest month (350 mm) and January the driest (<110 mm).

Vegetation resembles the *Kelat-Kendondong* forest type described by Wyatt-Smith (1963). Two principal soil series are the *Kuala Brang* (Orthoxic Tropudult) and *Bungor* (Typic Paleudult). The former occupies 90% of the area; the latter 10% typically occurs at lower elevations (cf. Saifuddin *et al.*, 1991; Zulkifli *et al.*, 2000). These soils are derived from arenaceous rocks and argillaceaous sediments that were deposited during the Triassic period (Roe, 1951; Saifuddin *et al.*, 1991). A low-grade metamorphism converted the arenaceous deposits into quartzite, quartz mica schist and schistose grit; the argillaceous sediments were changed to mica schist and indurated shale. Soil properties from a 2 m profile examined along a road cut in BTEC3 are presented in Table I.

### Measurement locations

Most of our measurements were conducted in the 14·4 ha BTEC3 (Figure 1(c)). This catchment was initially logged during the early 1960s. During a 1999 logging campaign, high-value trees were removed. Crawler tractors transported



DOI: 10.1002/esp

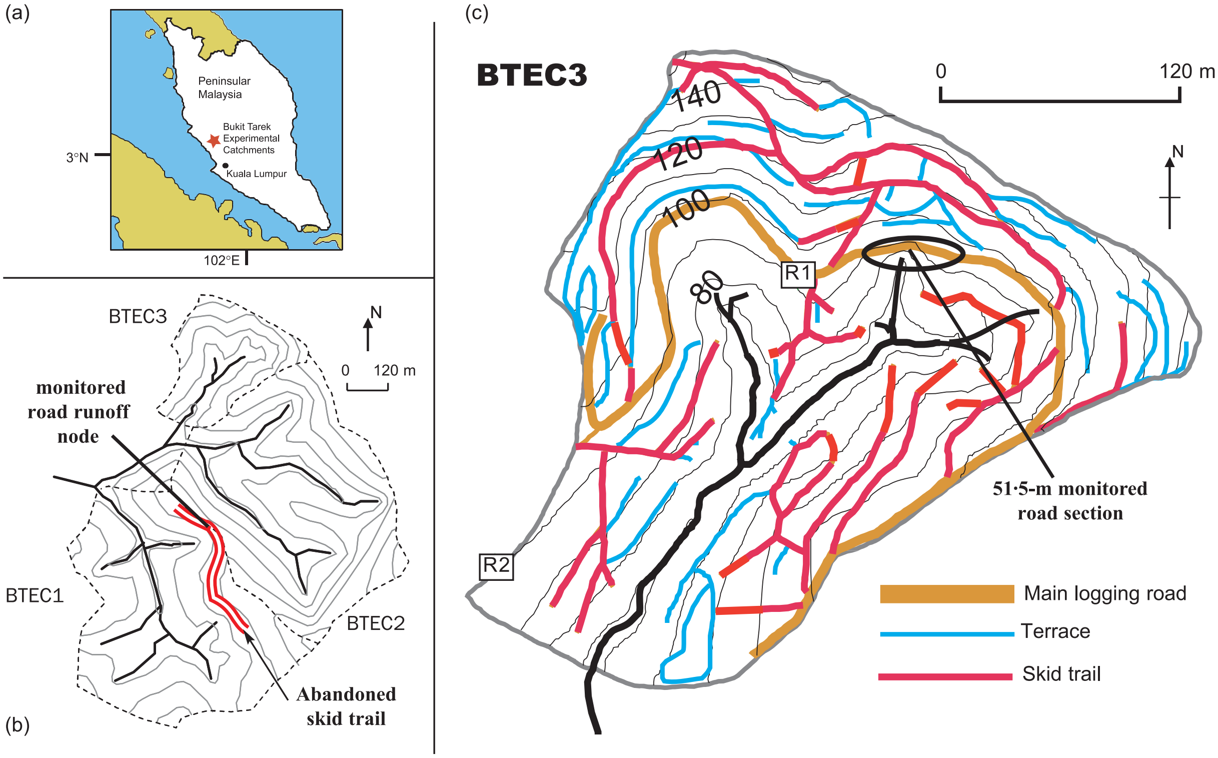


**Figure 1.** (a) Location of Bukit Tarek Experimental Catchment (BTEC) research site in Peninsular Malaysia; (b) locations of BTEC experimental catchments 1 and 3 (BTEC1, BTEC3); (c) locations of various types of road in BTEC3; skid trails were created for logging activities in 1999; terraces were created during the 2004 logging; the main logging road dates to the 1960s. R1 and R2 refer to the initial and supplementary rain gauge locations, respectively. The locations of monitored road sections in BTEC1 and BTEC3 are shown in (b) and (c). This figure is available in colour online at www.interscience.wiley.com/journal/espl

**Table I.** Depth-specific soil physical properties in BTEC3 (Ziegler *et al.*, 2006)

| Horizon[a] Extent (cm) | A 0–3 | $B_{t1}$ 3–32 | $B_{t2}$ 32–57 | $B_{t3}$ 57–71 | $B_{t4}$ 71–90 | $B_{w5}$ 90–110 | $C_r$ 110–130+ |
|---|---|---|---|---|---|---|---|
| $K_s$ (mm h$^{-1}$)[b] | ≥189 | 189 | 33 | 16 | 8 | 4 | ≤4 |
| $\rho_d$ (g cm$^{-3}$)[c] | 0·77 | 0·87 | 1·20 | 1·38 | 1·59 | 1·63 | — |
| Sand (%) | 40 | 39 | 40 | 41 | 47 | 60 | 56 |
| Silt (%) | 22 | 19 | 10 | 15 | 17 | 22 | 19 |
| Clay (%) | 38 | 43 | 49 | 44 | 36 | 18 | 24 |
| Rock content (%)[d] | <1 | <1 | <1 | 30–50 | 40–60 | >50 | saprolite |
| Color (dry) | 10YR5/3 | 10YR7/4 | 10YR8/6 | 10YR7/6 | 7·5YR7/6 | 7·5YR6/8 | 10YR8/4 |

[a] Subscripts of $B_t$ and $B_w$ refer to clay-rich and weathered B horizons, respectively; $C_r$ is saprolite.
[b] Saturated hydraulic conductivity, determined via well permeameter.
[c] Bulk density determined from a 90 cm$^3$ core.
[d] All rock material was highly weathered; gravel and pebbles were predominately quartz; fragments resembled the underlying bedrock.

cut logs from hillslopes to landings via a dense network of skid trails – about 2300 m in length or 16 km km$^{-2}$ for BTEC3 (Figures 1(b), 2(e) and 3(d)). The remaining unmerchantable forest was clear-cut from December 2003 to January 2004. The primary felling method in the upper catchment was uprooting or felling trees with a backhoe arm and scoop (Figure 2(d)). This method of removal required the creation of an additional 1806 m of skid trails – referred to as 'terraces' because of their ostensibly low impacts and because they served as locations for tree replanting following logging.



DOI: 10.1002/esp


**Figure 2.** (a) Exposed saprolite and bedrock on the main road in BTEC3; (b) pedestal erosion features (3–6 cm) on exposed side-cast material on road and trail surfaces in BTEC3; (c) overland flow resulting from HOF and ISSF at a monitored section on the main logging road in BTEC3; (d) backhoe situated on a skid trail in BTEC3 during logging in December 2004; (e) east hillslope of BTEC3 approximately 9 months following logging; despite the emergence of ferns (*Dicranopteris curranii*) and other pioneering shrubs, the extensive network of skid trails and terraces can be seen. This figure is available in colour online at www.interscience.wiley.com/journal/espl

In February 2004 we measured $K_s$ at 58 locations on the following four types of road and skid trail (Figure 1).

1. *Main logging road*: the principal 690 m road linking skid trails and logging landings in BTEC3 catchment (Figure 3(c)). This is the largest and most heavily traveled road in BTEC, with a median width of 3·49 m (Table II).
2. *Skid trails*: 2300 m of roads in BTEC3 constructed by bulldozers in 1999, then later reopened in 2003/2004 to facilitate hillslope logging operations (Sidle *et al.*, 2004) (Figure 3(a)).
3. *Terraces*: more than 1800 m of relatively low-use skid trails that were constructed in BTEC3 in 2003/2004, generally along contours, to allow backhoe access to hillslope logging areas (Figure 3(d)).
4. *Abandoned skid trail*: a skid trail used for logging operations in nearby BTEC1 catchment (Figure 1) roughly 40 years ago (Figure 3(b)). At the time of this study, dense understory vegetation and medium-sized trees were growing on this recovered surface, which had not been used since abandonment (Noguchi *et al.*, 2005).

In general, no type of road was designed to mitigate potential runoff or erosion impacts. For example, inboard ditches were not used to prevent surface runoff from flowing onto unprotected hillslopes; and road/trail surfaces were not treated with rock/gravel surfaces to reduce erosion.

At the height of operations the main logging road probably received about 10–20 passes per day from lorries for roughly two months. Trafficking on most skid trails by backhoes was generally limited to 2–5 days. Some trails were



DOI: 10.1002/esp

**Figure 3.** Examples of the four following road/trail types considered herein are shown: (a) an active skid trail, joining the main road from the upper left; (b) a former skid trail abandoned 40 years ago following logging; (c) the main logging road; (d) a newly constructed terrace (foreground), which is characterized by relatively shallow excavation into the hillslope. In (e), coauthor JNN is performing a $K_s$ experiment (0·25 m depth) on the main road with the compact constant head permeameter. This figure is available in colour online at www.interscience.wiley.com/journal/espl

**Table II.** Road/trail surface properties and dimensions for four types of road investigated

| | | Road type | | | |
|---|---|---|---|---|---|
| **Variable** | **Units** | **Main logging road** | **Skid trails** | **Terraces** | **Abandoned skid trail** |
| $K_{s\_0{\cdot}0m}$ | mm $h^{-1}$ | 0·8 ± 0·2 a | 2·0 ± 1·2 a | 34·0 ± 32·6 b | 61·9 ± 47·9 b |
| $K_{s\_0{\cdot}25m}$ | mm $h^{-1}$ | 1·7 ± 1·2 a | 2·5 ± 1·9 a | 2·7 ± 2·1 a | 5·5 ± 4·9 a |
| $\rho_b$ | Mg $m^{-3}$ | 1·48 ± 0·06 c | 1·28 ± 0·14 b | 1·17 ± 0·14 b | 0·80 ± 0·13 a |
| Slope | m $m^{-1}$ | 0·10 ± 0·05 a | 0·17 ± 0·08 b | 0·19 ± 0·10 b | 0·16 ± 0·08 b |
| $w$ | m | 3·49 ± 0·36 b | 3·18 ± 0·12 b | 3·35 ± 0·30 b | 2·70 ± 0·22 a |
| $d_L$ | m | 1·08 ± 0·20 c | 0·76 ± 0·32 ab | 0·46 ± 0·27a | 0·66 ± 0·11 ab |
| $d_{CB}$ | m | 3·00 ± 0·65 b | 1·55 ± 0·60 a | 1·03 ± 0·22 a | 1·25 ± 0·35 a |
| $n$ | – | 10 | 23 | 11 | 14 |
| Length (BTEC3)[†] | M | 690 | 2300 | 1806 | – |

$K_s$ is saturated hydraulic conductivity in the near surface (0·0–0·05 m) or at 0·25 m; $\rho_b$ is bulk density in the upper 5 cm (90 $cm^3$ cores); slope is for the running surface; $w$ is the width of the running surface; $d_L$ is the average depth of lowering of the road into the soil profile; $d_{CB}$ is the depth of the cutbank and $n$ is the sample number. The abandoned skid trail length is not listed because it is in a different catchment (BTEC1). Values are medians ± median absolute deviation (MAD). Treatments in the same *row* with the same letters are *not* considered significantly different (based on Kruskal–Wallace test, followed by comparison of box plots).

[†] Negishi *et al.* (2006).

more heavily used because they were arteries linking trails built along the hillslope contour. Trafficking on the terraces was at the low end of that for skid trails. Following the cessation of logging operations in January 2004, no vehicular traffic occurred on either skid trails or terraces. At the time of measurement, the main logging road received two or fewer four-wheel drive vehicle passes per day. We have no information on the level of use of the abandoned skid trail during prior logging efforts; we assume it was comparable to that of the most recent operations.

## Methods

### Rainfall

Rainfall was measured from November 2002 to December 2004 with an Onset (Pocasset, MA) 20·3 cm diameter tipping bucket rain gauge and Hobo logger. The initial location of the rain gauge was an open area in BTEC3, but it was moved in December 2003 to a nearby location to avoid logging operations (Figure 1(c)). Storms were defined as events if rainfall was 5 mm or more with no rain-free periods for more than 1 h (Negishi *et al.*, 2006; Ziegler *et al.*, 2006).

### Road dimensions and other properties

All roads and skid trails in BTEC3 were mapped with GPS (10 m accuracy), and road lengths were calculated from the GPS coordinates. For each road type considered, measurements were made at ten or more locations. These sites were chosen arbitrarily, without consideration to slope or total length of a particular road type, to capture the spatial variability throughout the basin and provide enough data for inter-comparison (i.e. at least 10 measurements per road type).

The following physical variables were determined: bulk density ($\rho_b$) of the upper 5 cm surface soil; slope gradient of the road running surface ($S$), width of the running surface ($w$), vertical depth of the cutbank ($d_{CB}$) and depth of surface lowering ($d_L$). Lowering refers to the depth to which the roads were excavated vertically into the hillslope profile, which was determined by identifying the depth on the road cut face that corresponded with the center of the road (based on hillslope geometry and slope). The maximum depth of lowering occurred at the base of the cutbank (i.e. $d_{CB}$). Slope was determined with a hand-held clinometer over a 10 m distance. Bulk density was determined from 90 cm$^3$ cores taken in the upper 5 cm near the centerline of the road, where $K_s$ was also measured.

### $K_s$ measurements

Two methods were used to measure $K_s$ with a field-based, constant-head permeameter (Amoozimeter; Amoozegar, 1992). The procedure used for measuring $K_s$ at the 0·25 m depth ($K_{s\_0{\cdot}25m}$) is referred to as the constant-head well permeameter technique, shallow well pump-in technique or borehole permeameter method (Amoozegar and Warrick, 1986). Water flowing from the Amoozimeter was monitored as it infiltrated into the soil within an augered column. Measurements were conducted until steady-state flow ($Q$) was observed. Saturated hydraulic conductivity was calculated using the Glover solution (Amoozegar, 1989):

$$K_s = Q\left[\frac{\sin h^{-1}(H/r) - ((r/H)^2 + 1)^{0.5} + r/H)}{2\pi H^2}\right] \tag{1}$$

where $H$ is the depth of water (i.e. the hydraulic head) in the augered hole with a radius $r$. During the experiments conducted in February and October of 2004, $H$ ranged from 14 to 15 cm; $r$ was 2·65 cm. Stream water was used in all measurements; water temperature varied from 24 to 27 °C.

Saturated hydraulic conductivity for the upper 0·05 m near-surface soil profile ($K_{s\_0{\cdot}0m}$) was determined via Darcy's law from experiments monitoring flow ($Q$) through 90 cm$^3$ soil cores under a constant input head:

$$K_s = \frac{QL}{\Delta hA} \tag{2}$$

where $L$ is the length that water flows through the core (5 cm), $A$ is the surface area of the core (18 cm$^2$) and $\Delta h$ is the difference between the input head and the head on the outflow side of the core. A constant input head (20–25 cm) was maintained using the Amoozimeter.



DOI: 10.1002/esp

## Statistical analysis

Preliminary analyses with the Shapiro–Wilks test suggested that the $K_s$ data did not follow a normal distribution. We therefore used the nonparametric Kruskal–Wallace (KW) test to explore differences in $K_s$ and other physical variables, such bulk density. When significant differences were identified, we grouped treatments by considering the following: (1) detailed box plots as the data summary; (2) the median as the estimator of central tendency; (3) the median absolute deviation (MAD) as the estimator of scale; (4) 95% confidence intervals about the median.

## Alteration index

An alteration index ($\Delta P$) was calculated for both bulk density and $K_s$ to show percentage change in values on road/skid trail surfaces relative to undisturbed control surfaces:

$$\Delta P = \frac{P_{\text{disturbed}} - P_{\text{control}}}{P_{\text{control}}} \times 100\% \tag{3}$$

where $P_{\text{disturbed}}$ is the property value on the road and $P_{\text{control}}$ is the value on undisturbed surfaces, which were located in the adjacent BTEC1 (Ziegler *et al.*, 2006).

## Monitoring of road HOF during storms

We installed two v-notch weirs (0·6 m × 0·6 m × 0·9 m) on one section on the main logging road where flow discharged into hillslope gullies (Figures 1(c) and 2(c)). Slope of this section was 0·11 m $m^{-1}$. Galvanized zinc sheeting was cemented to exposed bedrock to direct flow from the road into the weirs (Figure 2(c); a detailed diagram is presented by Negishi *et al.*, 2006). Flow rates were monitored continuously at 2–3 min intervals using WT-HR water level sensors (TruTrack, NZ) situated in the drop box weirs. At a runoff node draining one 30 m section of the abandoned skid trail in BTEC1 we use galvanized zinc sheeting to channel flow from the road into a tipping bucket measurement apparatus (Figure 1(b)). Flow rate was determined from tip rates that were recorded with a Hobo data logger.

To distinguish between HOF and ISSF we assumed that any road runoff occurring 20 min after the cessation of precipitation was ISSF. This conservative 20 min criterion for stormflow separation was determined by measuring the time following rainfall cessation until runoff cessation for several events that generated HOF only (Negishi *et al.*, 2006). Additionally, ISSF inputs were easily detected by sudden increases of specific conductance (from <15 to >30 μS $cm^{-1}$). Flow rates measured separately at both weirs on the main logging road were combined to obtain a single storm flow hydrograph because the two road sections were hydrologically connected. HOF was expressed as a depth by dividing by road running surface area: 183 $m^2$ for the main logging road; 81 $m^2$ for the abandoned skid trail (Negishi, 2005).

## KINEROS2

To ascertain the propensity of each road type to generate Hortonian overland flow, we conducted diagnostic computer simulations using the KINEROS2 runoff model (Smith *et al.*, 1995, 1999). Overland flow in KINEROS2 is treated as a one-dimensional flow process, in which discharge per unit width ($Q$) is expressed in terms of water storage per unit area through the kinematic approximation:

$$Q = \alpha h^m \tag{4}$$

where $\alpha$ and $m$ are parameters related to slope, surface roughness and flow condition (laminar or turbulent) and $h$ is water storage per unit area. Equation (4) is used in conjunction with the continuity equation:

$$\frac{\partial h}{\partial t} + \frac{\partial Q}{\partial x} = q(x,t) \tag{5}$$

where $x$ is distance downslope, $t$ is time and $q(x, t)$ is net lateral inflow rate per unit length of channel. Solution of Equation (5) requires estimates of time- and space-dependent rainfall $r(x, t)$ and infiltration $f(x, t)$ rates:

$$q(x,t) = r(x,t) - f(x,t) \tag{6}$$

Infiltrability is defined as the limiting rate at which water can enter the soil surface (Hillel, 1971). Modeling of this process utilizes several input parameters that describe the soil profile: e.g., $K_s$, integral capillary drive or matric potential ($G$), porosity and pore size distribution index. The general infiltrability ($f_c$) equation is a function of cumulative infiltrated depth ($I$) (following Parlange *et al.*, 1982):



DOI: 10.1002/esp

$$f_c = K_s\left[1 + \frac{a}{e^{(aI/B)} - 1}\right] \tag{7}$$

where $a$ is a constant related to soil type (assumed to be 0·85 unless otherwise specified) and $B = (G + h_w)(\theta_s - \theta_i)$, for which $h_w$ is surface water depth (computed internally) and the second term, unit storage capacity, is the difference of saturated ($\theta_s$) and initial ($\theta_i$) volumetric moisture contents (i.e. $\Delta\theta_i = \theta_s - \theta_i$). The expression ($\theta_s - \theta_i$) is calculated as $\phi(S_{max} - S_i)$, where $\phi$ is porosity and $S_{max}$ and $S_i$ are respectively the maximum and initial values of 'relative saturation', defined as $S = \theta/\phi$, or the fraction of the pore space filled with water. Antecedent soil moisture is parameterized by assigning event-dependent values of relative saturation. Infiltration can be modeled in as many as two soil layers (e.g. to incorporate the effects of a flow-restricting layer).

## HOF Simulations

One purpose of the diagnostic simulations using KINEROS2 was to explore plausible differences in the propensity of each of the four types of road to generate HOF. We first calibrated the model to simulate HOF on the 183 $m^2$ section of the main logging road during five monitored storms (discussed below). We tested the model using data from five different storms. We then selected 17 other monitored rainfall events for simulation of HOF on all roads (Table III). To ensure a large range in application, we initially chose storms with either the highest or lowest values of the total precipitation, duration and maximum sustained rainfall intensity (1, 10, 30, 60 min). Five additional storms were selected to complete the range from small to large events in terms of total rainfall depth.

**Table III.** Characteristics of five calibration (c), five evaluation (e) and 17 HOF simulation storms

| Storm | Start m/d/y h:min | End m/d/y h:min | RF mm | Duration min | $I_{1\_MAX}$ mm $h^{-1}$ | $I_{10\_MAX}$ mm $h^{-1}$ | $I_{30\_MAX}$ mm $h^{-1}$ | $I_{60\_MAX}$ mm $h^{-1}$ |
|---|---|---|---|---|---|---|---|---|
| **Calibration–evaluation storms** | | | | | | | | |
| **c-1** | 12/2/2002 17:22 | 12/2/2002 18:16 | 7·3 | 54 | 40 | 20 | 13 | na |
| **c-2** | 12/3/2002 15:07 | 12/3/2002 15:54 | 24·2 | 47 | 100 | 84 | 44 | na |
| **c-3** | 7/8/2003 3:07 | 7/8/2003 3:32 | 8·4 | 25 | 90 | 38 | na | na |
| **c-4** | 9/7/2003 14:56 | 9/7/2003 15:43 | 5·6 | 46 | 40 | 24 | 9 | na |
| **c-5** | 9/19/2003 5:54 | 9/19/2003 10:07 | 5·7 | 253 | 20 | 4 | 4 | 3 |
| **e-1** | 12/4/2002 15:59 | 12/4/2002 17:07 | 10·6 | 68 | 40 | 26 | 15 | 10 |
| **e-2** | 2/9/2003 17:11 | 2/9/2003 17:29 | 17·1 | 18 | 120 | 84 | na | na |
| **e-3** | 6/22/2003 0:22 | 6/22/2003 2:13 | 5·5 | 111 | 30 | 6 | 5 | 3 |
| **e-4** | 6/22/2003 16:34 | 6/22/2003 19:29 | 8·5 | 175 | 30 | 16 | 7 | 4 |
| **e-5** | 10/6/2003 18:54 | 10/6/2003 21:00 | 5·6 | 126 | 20 | 6 | 5 | 4 |
| **Simulated storms** | | | | | | | | |
| **1** | 5/2/03 15:48 | 5/2/03 22:17 | 127 | 389 | 180 | 144 | 109 | 71 |
| **2** | 9/25/03 3:23 | 9/25/03 7:25 | 91 | 242 | 80 | 66 | 59 | 52 |
| **3** | 3/18/03 16:31 | 3/18/03 17:20 | 84 | 49 | 160 | 146 | 130 | na |
| **4** | 4/29/04 14:43 | 4/29/04 16:43 | 81 | 120 | 200 | 142 | 104 | 74 |
| **5** | 11/5/04 16:03 | 11/5/04 18:10 | 79 | 127 | 160 | 102 | 77 | 56 |
| **6** | 1/28/04 15:45 | 1/28/04 23:01 | 70 | 437 | 90 | 66 | 57 | 41 |
| **7** | 5/6/03 17:43 | 5/6/03 18:51 | 64 | 68 | 160 | 104 | 78 | 63 |
| **8** | 11/28/04 16:00 | 11/28/04 21:58 | 57 | 358 | 100 | 64 | 53 | 42 |
| **9** | 12/19/04 16:18 | 12/19/04 20:52 | 45 | 274 | 100 | 72 | 48 | 34 |
| **10** | 8/29/03 7:25 | 8/29/03 8:23 | 32 | 58 | 80 | 70 | 56 | 32 |
| **11** | 11/23/03 19:00 | 11/23/03 20:37 | 25 | 97 | 80 | 38 | 31 | 23 |
| **12** | 7/21/03 10:04 | 7/21/03 13:09 | 20 | 186 | 60 | 45 | 30 | 17 |
| **13** | 4/12/03 14:08 | 4/12/03 15:21 | 16 | 73 | 80 | 52 | 25 | 15 |
| **14** | 10/20/03 3:48 | 10/20/03 5:11 | 13 | 83 | 40 | 28 | 18 | 11 |
| **15** | 12/13/02 15:50 | 12/13/02 15:58 | 7 | 8 | 100 | na | na | na |
| **16** | 11/30/03 16:45 | 11/30/03 17:57 | 6 | 72 | 20 | 16 | 11 | 6 |
| **17** | 10/6/03 16:12 | 10/6/03 20:06 | 5 | 234 | 20 | 4 | 3 | 2 |

RF is total rainfall depth; $I_{1\_MAX}$, $I_{10\_MAX}$, $I_{30\_MAX}$ and $I_{60\_MAX}$ refer to maximum 1, 10, 30 and 60 min rainfall intensities; 'na' indicates the event was too short to have a sustained intensity of the specified length.



DOI: 10.1002/esp

**Table IV.** Parameters used in KINEROS2 diagnostic overland flow simulations

| Parameter | Units | Road/trail type | | | |
|---|---|---|---|---|---|
| | | Main logging road | Skid trail | Terrace | Abandoned skid trail |
| $K_s$ (layer 1) | mm h$^{-1}$ | 0·5 | 1·3 | 22·8 | 19·4 |
| $K_s$ (layer 2) | mm h$^{-1}$ | 1·1 | 1·7 | 1·8 | 3·7 |
| $C_vK_s$ | – | 0·25 | 0·60 | 0·96 | 0·77 |
| $G$ (layer 1) | mm | 75 | 77 | 123 | 115 |
| $G$ (layer 2) | Mm | 77 | 78 | 78 | 82 |
| Porosity | – | 0·35 | 0·45 | 0·52 | 0·45 |
| Rock | – | 0·50 | 0·40 | 0·10 | 0·30 |
| Manning's $n$ | – | 0·105 | 0·14 | 0·245 | 0·35 |
| Relief | mm | 2 | 5 | 10 | 10 |
| Spacing | m | 2 | 1 | 1 | 2 |

The depth of soil layer 1 was 0·5 m. $C_vK_s$, the coefficient of variation of $K_s$, was calculated as MAD/median (Table II). Common parameters used for all simulations include the following: (i) particle density = 2·49 Mg m$^{-3}$ ($n$ = 10 measurements) and (ii) pore size distribution index = 0·25 (Rawls *et al.*, 1982). Relief and spacing values are based on observations.

Simulations for the other three road types were performed by replacing parameters for the main logging road with those associated with skid trails, terraces and the abandoned skid trail (Table IV). Saturated hydraulic conductivity was determined from field measurements, and other key parameters, such as porosity and Manning's $n$, were based on published data for sandy clay loam soils (Rawls *et al.*, 1982; Woolhiser *et al.*, 1990; Morgan, 1995). We estimated capillary drive ($G$) via back-calculation using the following equation involving sorptivity ($S$) and $K_s$ (Smith *et al.*, 2002):

$$G = \frac{0.5S^2}{K_s} \tag{8}$$

where the constant 0·5 is based on the assumption that the advancing water front moves as a square pulse of constant water content (cf. White and Sully, 1987). We used our measured near-surface $K_s$ and $\rho_b$ data and the $\rho_b$-versus-$S$ relationship for compacted forest soils reported by Gardner and Chong (1990). The resulting $G$ estimates were further adjusted during model calibration.

Because we collected $K_s$ at two soil depths, we simulated a two-layer soil profile for each road/skid trail surface. Simulation time step was 1 min, matching the temporal resolution of the rainfall record; the simulation time was one hour longer than the storm duration. The assigned antecedent soil moisture value ($S_i$ = 0·5) was slightly below field capacity (0·67 for sandy clay loam). The canopy interception depth was assumed negligible on the main logging road, skid trails and terraces; this represents the clear-cut landscape immediately following logging. Keeping these parameters constant allowed us to isolate HOF generation patterns caused by differences in measured soil properties – most importantly, $K_s$. Interception and canopy cover for the abandoned skid trail, which represented a scenario of a 40 year recovery, were based initially on observations during prior studies (Noguchi *et al.*, 2005; Negishi, 2005), then adjusted during model calibration (7 mm and 80%, respectively).

# Results

## Rainfall

During the 25 month measurement period, 264 storms were recorded (Negishi, 2005). Median values for total storm rainfall and storm duration were 16 mm and 83 min, respectively. Half of the recorded 1 min rainfall intensity values were 80 mm h$^{-1}$ or more (Figure 4). The absolute maximum 1, 5, 10, 20, 30 and 60 min intensities for all storms were 200, 164, 146, 136, 130 and 74 mm h$^{-1}$, respectively. The median maximum sustained 1, 5, 10, 20, 30 and 60 min intensities were 80, 56, 45, 32, 25 and 17 mm h$^{-1}$ (Ziegler *et al.*, 2006). Cumulative density functions for total storm rainfall depth, maximum 1 min rainfall intensity and storm duration are shown in Figure 4.



DOI: 10.1002/esp

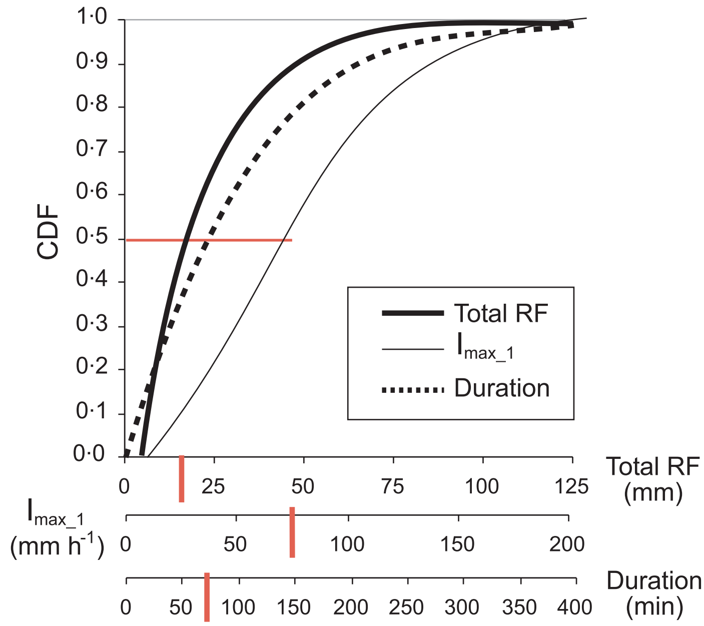


**Figure 4.** For 264 storms the cumulative probability density functions (CDFs) for total rainfall depth (mm), maximum 1 min rainfall intensity (mm $h^{-1}$) and event duration (min). The thick vertical line on each of the *x*-axes corresponds to a CDF value of 0·5. This figure is available in colour online at www.interscience.wiley.com/journal/espl

## Road/trail dimensions in BTEC3

Total road/trail length in BTEC3 was approximately 4800 m, partitioned among three road types as follows (Table II): 690 m (main logging road), 2300 m (skid trails) and 1806 m (terraces). The main logging road had the widest running surface ($w$ = 3·5 m) and the deepest cutbank ($d_{CB}$ = 3 m) and was the most deeply excavated into the hillslope profile ($d_L$ > 1 m). Median slopes on the running surface of each road type were not greatly different (Table II). This similarity may be related to our sampling scheme, for which measurement density on each type of road was different. The median value for skid trails disguises the fact that the slopes of some across-contour trails accessing others built parallel to the contour were quite steep (>0·40 m $m^{-1}$; see Figure 3(a), (d)). An important difference among all types of road was the depth of excavation: main logging road (1·08 m) > skid trails (0·76 m) > terraces (0·46 m). Compared with the abandoned skid trail in BTEC1, the BTEC3 skid trails were slightly wider and excavated deeper into the hillslope profile (Table II).

The total road/skid trail length of 4800 m in BTEC3 equates to a density of about 33 km $km^{-2}$. The road network is also approximately seven times longer than the BTEC3 stream network. Based on median widths (Table II), the road/trail system occupied only 5·6% of the basin area. This is at the low end of percentages reported for other ground-based logging sites in Malaysia: e.g., 5–10% in Peninsular Malaysia (Baharuddin, 1988; Baharuddin and Abdul Rahim, 1994; Zulkifli and Anhar, 1994) and 4–24% in Sabah (Phillips, 1986; Malmer and Gripp, 1990; Pinard *et al.*, 2000). However, the area occupied by roads/trails exceeded 15–20% on the most densely roaded hillslopes in BTEC3 (Figures 2(e) and 3(c)).

## Road/trail bulk density

Bulk density ($\rho_b$) in the upper 5 cm was highest on the main logging road (1·48 Mg $m^{-3}$); the lowest bulk density (0·80 Mg $m^{-3}$) was associated with the abandoned skid trail (Table II). Bulk densities on the BTEC3 skid trails and terraces were not significantly different (1·28 versus 1·17 Mg $m^{-3}$). Compared with the adjacent undisturbed hillslope, bulk density on the main logging road was 100% higher (Table V). Bulk densities on skid trails and terraces were elevated by 75 and 60% compared with undisturbed sites. These increases are higher than those reported for other logging roads in Malaysia (13–60%; Table V). Bulk density on the abandoned skid trail was elevated by only 10%.



DOI: 10.1002/esp

**Table V.** Relative change in near-surface bulk density ($\rho_b$) and near-surface saturated hydraulic conductivity ($K_s$) for roads versus undisturbed surfaces at BTEC and other places in Peninsular Malaysia (PM) or Sabah

| Location | Road type | Excavation† | $\Delta\rho_b$ (%) | $\Delta K_s$ (%)†† |
|---|---|---|---|---|
| BTEC3 (PM)[1] | Main logging road | 1·08 m | 103 | −99 |
| BTEC3 (PM)[1] | Skid trail | 0·76 m | 75 | −99 |
| BTEC3 (PM)[1] | Terrace | 0·46 m | 60 | −95 |
| BTEC1 (PM)[1] | Abandoned skid trail | 0·66 m | 10 | −91 |
| **Other sites in Malaysia** | | | | |
| Jengka (PM)[2] | Road | minimal | 42 | −70 |
| Jengka (PM)[2] | Skid trail | minimal | 32 | −79 |
| Sipitang (Sabah)[3] | Track on clay | ≤1 m | 56 | −82 |
| Sipitang (Sabah)[3] | Track on sand | ≤1 m | 21 | −97 |
| Sg. Tekam (PM)[4] | Skid trail | minimal | 39 | −96 |
| Sg. Tekam (PM)[4] | Secondary road | minimal | 13 | −59 |
| Ula Segama (Sabah)[5] | Skid trail | – | 60 | −99 |
| Ula Segama (Sabah)[6] | Tractor tracks (12 years old) | minimal | 34 | −82 |

[1] This study, for which undisturbed control values used in the calculation of $\Delta\rho_b$ and $\Delta K_s$ (via Equation (3)) were 0·73 Mg m$^{-3}$ and 675 mm h$^{-1}$, respectively (for BTEC1, see Ziegler *et al.*, 2006); [2] Baharuddin (1995); [3] Malmer and Gripp (1990); [4] Kamaruzaman (1996); [5] Brooks and Spencer (1997); [6] Van der Plas and Bruijnzeel (1993).

† Excavation indicates either the depth of excavation into the hillslope profile or the degree to which it typically occurred.

†† Reported infiltration rates in other studies were converted to $K_s$ using Philip's (1957) equation (assuming time ($t$) is approaching infinity): $i = 0{\cdot}5St^{-0{\cdot}5} + 0{\cdot}5K_s$ (where S is sorptivity, Ziegler and Giambelluca, 1997).

## Road/trail $K_s$

Median near-surface $K_s$ values for both the main logging road (<1 mm h$^{-1}$) and the skid trails (2 mm h$^{-1}$) were significantly lower than for the terraces (34 mm h$^{-1}$), as well as the abandoned skid trail (62 mm h$^{-1}$) (Table II). Values for the latter three types of road/trail were similar to reported values for skid trails and secondary logging tracks/trails worldwide (Table VI). Compared with undisturbed surface soils (675 mm h$^{-1}$), the $K_s$ values for all the BTEC roads were two to three orders of magnitude lower (Table VI). The percent reductions in $K_s$ on roads versus the undisturbed control are at the extreme lower end of values obtained at other sites in Malaysia (Table V). Even the abandoned skid trail, where bulk density almost completely recovered, still had a near-surface $K_s$ value about 90% lower than on the adjacent forested hillslope.

**Table VI.** Synthesis of reported values for surface saturated hydraulic conductivity ($K_s$) on various types of unpaved road/trail and undisturbed control surface

| Main road | Primary skid trail | Secondary trails/tracks/paths | Log landing | Undisturbed surface | Location |
|---|---|---|---|---|---|
| <1 | 2 | 34 | – | >675 | BTEC3 (this study) |
| <1–23 | <1–24 | 10–69 | 4–142 | 33–360 | Sabah & P. Malaysia[1] |
| 3 | 13–32 | 16–28 | 3 | 32–575 | Australia[2] |
| <1–20 | 13–40 | 70–225 | 33 | 50–445 | USA & Canada[3] |
| 2–15 | – | 8–13 | – | 90–254 | SE Asia & Hawaii[4] |

The $K_s$ values (mm h$^{-1}$) are derived from various infiltrability variables (reported by the authors as percolation estimates, infiltration rates, infiltration capacities and steady-state infiltration rates) using Philip's (1957) equation (see footnote in Table V). The 675 mm h$^{-1}$ $K_s$ value for undisturbed surface in this study was determined in the adjacent BTEC1 (Ziegler *et al.*, 2006).

[1] Brooks *et al.* (1994); Kamaruzaman (1996); Baharuddin *et al.* (1996); Brooks and Spencer (1997); Malmer and Gripp (1990); Van der Plas and Bruijnzeel (1993); Malmer (1996); Chappell and Ternan (1997); Chappell (personal communication).

[2] Riley (1984); Rab (1996); Croke *et al.* (2001).

[3] Reinhart (1964); Perry (1964); Hatchell *et al.* (1970); Johnson and Beschta (1980); Luce and Cundy (1994), Reid and Dunne, 1984; Loague and Gander (1990); Commandeur and Wass (1994); Luce (1997).

[4] Ziegler and Giambelluca (1997); Ziegler *et al.* (2000); Ziegler *et al.* (2004); Ziegler and Sutherland (2006); Sutherland *et al.* (2001).



DOI: 10.1002/esp

**Table VII.** Results and error indices for KINEROS2 calibration (c events) and evaluation (e events) simulations of HOF on the monitored main logging road section

| | | Measured | | | KINEROS2 | | | | |
|---|---|---|---|---|---|---|---|---|---|
| Storm | Date | RF mm | RO mm | ROC – | SAT – | $E_{total}$ – | $E_{peak}$ – | ME – | *n* – |
| c-1 | 2 Dec 02 | 7·3 | 2·0 | 0·28 | 0·33 | 0·6 | 0·1 | 0·45 | 38 |
| c-2 | 3 Dec 02 | 24·2 | 18·4 | 0·76 | 0·60 | 0·1 | 0·0 | 0·91 | 29 |
| c-3 | 8 Jul 03 | 8·4 | 3·5 | 0·41 | 0·53 | 0·31 | 0·00 | 0·80 | 29 |
| c-4 | 7 Sep 03 | 5·6 | 0·9 | 0·16 | 0·40 | 1·9 | 0·3 | −0·86 | 27 |
| c-5 | 19 Sep 03 | 5·7 | 0·8 | 0·14 | 0·47 | −0·53 | −0·22 | 0·28 | 53 |
| e-1 | 4 Dec 02 | 10·6 | 5·0 | 0·47 | 0·72 | 0·18 | 0·35 | 0·56 | 49 |
| e-2 | 9 Feb 03 | 17·1 | 15·0 | 0·87 | 0·40 | −0·07 | −0·12 | 0·86 | 20 |
| e-3 | 22 Jun 03 | 5·5 | 1·3 | 0·24 | 0·78 | −0·04 | 0·14 | 0·44 | 104 |
| e-4 | 22 Jun 03 | 8·5 | 3·8 | 0·45 | 0·78 | 0·14 | 0·20 | 0·30 | 35 |
| e-5 | 6 Oct 03 | 5·6 | 1·7 | 0·30 | 0·85 | −0·30 | −0·26 | 0·30 | 56 |

RF is total rainfall; RO is total measured road HOF, ROC is the runoff coefficient (RO/RF); SAT is relative saturation; $E_{total}$, $E_{peak}$ and ME are total prediction error (Equation (9)), total error in predicted peak (Equation (10)) and model efficiency (Equation (11)), respectively; *n* is the number of observation values used in calculation of ME.

At a depth of 0·25 m below the surface, the range in median $K_s$ among the four road/skid trail types was only 1·7–5·5 mm h$^{-1}$, and there was no significant difference among these roads (Table II). The $K_{s\_0 \cdot 25m}$ values are more in line with the saturated hydraulic conductivity values found at or below 0·7 m in the soil profile (compare with Table I). This similarity is no coincidence, because all roads are excavated more than 0·5 m into the soil profile (Table II).

## Measured road HOF

Road runoff was measured during more than 90 storms, but only 10 events were identified where all runoff was HOF (Table VII). The other storms had complex hydrographs that resulted from mixing of ISSF, return flow from shallow pipes and/or road runoff from a prior event. Our selection of these HOF-only storms is more conservative than the procedure used earlier by Negishi *et al.* (2006) in BTEC3. Rainfall intensity variables associated with these storms are shown in Table III. These storms are identified with leading characters 'c' or 'e' to designate that they were used in the initial calibration or subsequent evaluation of KINEROS2, respectively. Total rainfall depth for these 10 storms ranged from 5·5 to 24·2 mm. Median measured road runoff coefficients (ROC = total HOF/total rainfall) was 0·36 (Figure 5; Table VII). The two largest events (17 and 24 mm) had ROC values greater than 0·75.

At the runoff collection node on the abandoned skid trail in BTEC1, no runoff was recorded for events with total rainfall depths less than 25 mm, and all detected road runoff was a mixture of HOF and ISSF. Therefore, we were not able to obtain HOF-only hydrographs for model calibration and testing for this skid trail. However, this finding was useful for constraining the model from predicting HOF for events with rainfall depth less than 25 mm.

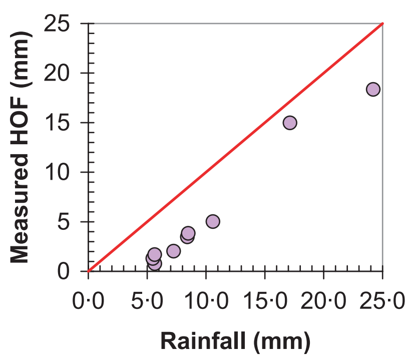


**Figure 5.** Total HOF (mm) measured during 10 storms at the monitored section on the main logging road.



DOI: 10.1002/esp

## KINEROS2 calibration

We used five observed storms to calibrate KINEROS2 to predict HOF on the monitored 183 $m^2$ section of the main logging road (c1–5, Table III). Calibration was performed by adjusting prescribed parameters to collectively reduce error as determined by the following three indices:

percent error in total estimate

$$E_{\text{total}} = \frac{(P_{\text{total}} - O_{\text{total}})}{O_{\text{total}}} \times 100 \tag{9}$$

percent error in peak value estimate

$$E_{\text{peak}} = \frac{(P_{\text{peak}} - O_{\text{peak}})}{O_{\text{peak}}} \times 100 \tag{10}$$

model efficiency (Nash and Sutcliffe, 1970)

$$\text{ME} = 1 - \left( \frac{\sum_{i=1}^{n}(O_i - P_i)^2}{\sum_{i=1}^{n}(O_i - \bar{O})^2} \right) \tag{11}$$

where $P_{\text{total}}$ and $O_{\text{total}}$ are predicted and observed total storm discharges, $P_{\text{peak}}$ and $O_{\text{peak}}$ are predicted and observed peak discharges, $P_i$ and $O_i$ are predicted and observed instantaneous discharge rates and $\bar{O}$ is the mean of the observed values. Notable adjustments to model parameters during calibration were reductions of measured $K_s$ and assigned $G$ values by one-third, increasing the layer 1 soil depth to 0·5 m and adjustment of the abandoned skid trail interception and cover values (Table IV).

The error indices show a wide range of prediction skill for five evaluation events (Table VII). The smallest storms had the lowest ME values, indicating generally poor simulation of the HOF hydrographs. In fact, the lowest ME value was for calibration event c-4 (ME = –0·86). Negative ME values indicate the simulation was worse than simply taking the mean of observed values. The largest simulated storm (c-2, 24·2 mm) had an ME = 0·91 (Table VII, Figure 6). Perfect agreement between observed and simulated values results in an ME of 1.

Because it was not possible to produce a good fit for the entire range of events during calibration, we placed more importance on reducing errors for the largest events. Inability of the model to fit small-scale variations in observed hydrographs during some storms may be related to differences in rainfall measured at the gauge and that actually falling on the monitored road section (Figure 6). Nevertheless, the error and model fit values associated with KINEROS2-prediction of HOF for the five evaluation events were operationally acceptable: $-0{\cdot}30 \le E_{\text{total}} \le 0{\cdot}18$; $-0{\cdot}26 \le E_{\text{peak}} \le 0{\cdot}35$ and $0{\cdot}30 \le \text{ME} \le 0{\cdot}86$ (Table VII).

## Simulation of HOF

Runoff coefficients for the 17 simulations of HOF on the main logging road and skid trails were above 0·50 for all events with more than 15 mm of rainfall (Figure 7). For large events (>50 mm), ROCs ranged from 0·69 to 0·94 (Figure 7). Even for the 6 mm ($I_{1\_MAX}$ = 20 mm $h^{-1}$) event 16, ROCs on the main logging road and skid trails were over 0·20 (not shown). Simulated HOF on terraces was slightly lower than that on the main logging road and skid trails (Figure 7). Total runoff on the three types of BTEC3 road/trail increased with increasing depth of rainfall, approaching limits of about 90% for the largest events (Figure 7). HOF was not simulated on the abandoned skid trail for events smaller than 25 mm; this is consistent with our observations on the monitored road section in BTEC1.

Of the 822 mm of rainfall that fell during the 17 simulated storms, an estimated 5330 $m^3$ of HOF was simulated on the 4796 m road/trail network in the 14.4 ha catchment (Table VIII). This is equivalent to a depth of 37 mm – or approximately 4% of the total rainfall. For this estimate, basin total HOF was extrapolated from the road-segment-scale simulations (183 $m^2$) by multiplying by appropriate road width and basin length conversion factors (i.e. based on Table II). About 45% of the simulated flow was generated on skid trails, compared with 32 and 23% for the main logging road and terraces. The estimated skid trail contribution is greater primarily because of the higher total road length.



DOI: 10.1002/esp

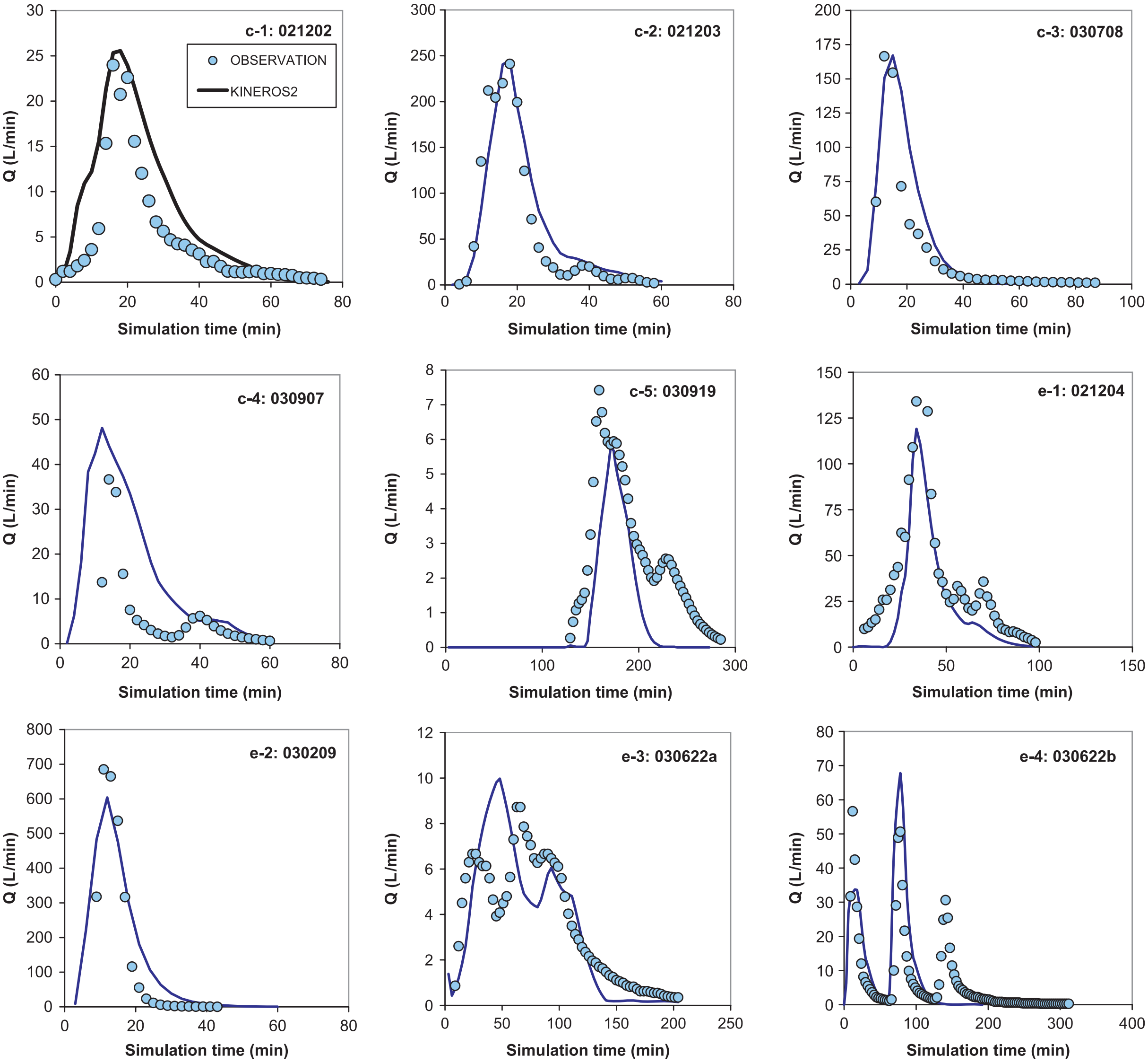


**Figure 6.** Observed (circle) and KINEROS2-predicted (line) HOF for nine monitored storms. The first five storms are the calibration (c) events; the others are evaluation (e) events. Error indices are presented in Table VII. This figure is available in colour online at www.interscience.wiley.com/journal/espl

# Discussion

## Validity of measurements

Values of $K_s$ reported for roads/trails worldwide range from less than 1 mm $h^{-1}$ on main roads to more than 200 mm $h^{-1}$ on various types of secondary trail (Table VI). Measured BTEC3 road $K_s$ data show a similar general relationship, i.e. main roads < skid trails < secondary trails (i.e. terraces) < undisturbed land covers (Table VI). Variations in $K_s$ for any type of the road/trail shown do not simply reflect differences in degree of compaction by heavy machinery during road construction and subsequent traffic; they also represent differences in soil type, surface conditions when compaction occurred (e.g. soil moisture) and $K_s$ measurement techniques (e.g. rainfall simulation versus infiltrometer versus disk permeameter). Importantly, the variation is also related to the excavated depth of the road surface within the hillslope profile and the properties of the subsurface material at these depths. At BTEC3, most of the roads and trails are excavated



DOI: 10.1002/esp

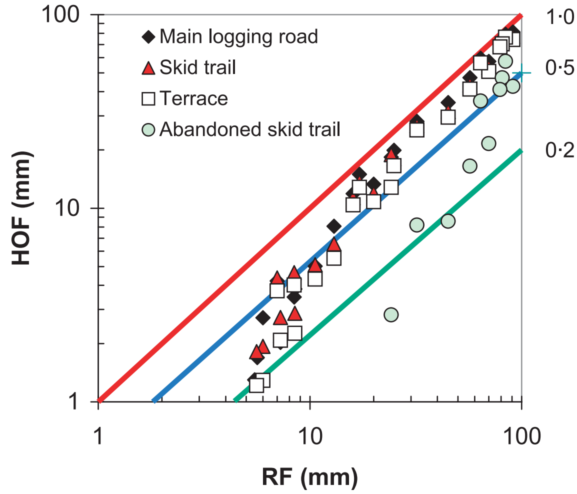


**Figure 7.** Simulated HOF for the calibration, evaluation and simulated storms for the main logging road, skid trails, terraces and the abandoned skid trail. The lines represent runoff coefficients of 1·0, 0·5 and 0·2. This figure is available in colour online at www.interscience.wiley.com/journal/espl

**Table VIII.** KINEROS2-predicted HOF on three types of road/trail in BTEC3 during 17 selected storm events

| Storm | RF mm | Main logging road $m^3$ | Skid trails $m^3$ | Terraces $m^3$ | All roads $m^3$ | $ROC_{basin}$ – | Recovered $m^3$ | Reduction % |
|---|---|---|---|---|---|---|---|---|
| 1 | 127 | 278 | 394 | 200 | 872 | 0·05 | 540 | 38% |
| 2 | 91 | 196 | 275 | 138 | 609 | 0·05 | 334 | 45% |
| 3 | 84 | 191 | 278 | 142 | 611 | 0·05 | 450 | 26% |
| 4 | 81 | 180 | 258 | 131 | 570 | 0·05 | 370 | 35% |
| 5 | 79 | 175 | 250 | 127 | 552 | 0·05 | 321 | 42% |
| 6 | 70 | 138 | 190 | 95 | 423 | 0·04 | 169 | 60% |
| 7 | 64 | 143 | 206 | 105 | 455 | 0·05 | 281 | 38% |
| 8 | 57 | 114 | 154 | 77 | 345 | 0·04 | 129 | 63% |
| 9 | 45 | 85 | 113 | 55 | 252 | 0·04 | 67 | 73% |
| 10 | 32 | 68 | 95 | 47 | 210 | 0·05 | 64 | 69% |
| 11 | 25 | 48 | 64 | 31 | 143 | 0·04 | 4 | 97% |
| 12 | 20 | 32 | 42 | 20 | 95 | 0·03 | 0 | 100% |
| 13 | 16 | 29 | 40 | 19 | 88 | 0·04 | 0 | 100% |
| 14 | 13 | 19 | 23 | 10 | 53 | 0·03 | 0 | 100% |
| 15 | 7 | 10 | 16 | 7 | 33 | 0·03 | 0 | 100% |
| 16 | 6 | 7 | 7 | 2 | 16 | 0·02 | 0 | 100% |
| 17 | 5 | 0 | 0 | 0 | 0 | 0·00 | 0 | 100% |
| **Total** | 822 | 1712 | 2407 | 1207 | 5326 | 0·04 | 2729 | 49% |

RF is total rainfall depth for each of the 17 non-calibration/validation events (Table II). Each 'All-roads' value is the sum volume of runoff on the main logging road, skid trails and terraces. $ROC_{basin}$ is the basin runoff coefficient (all roads HOF/basin-wide rainfall volume). 'Recovered' is total simulated road HOF for the scenario that all roads/trails have recovered to the current level of the abandoned skid trail. 'Reduction' is the percentage decrease between all-road HOF and that for the recovered scenario.

to a depth of at least 0·5–1 m into consolidated subsurface material with naturally low $K_s$ (Figure 8). As shown in Table I, $K_s$ decreases from 16 to 4 mm $h^{-1}$ between the depths of 0·5 and 1·3 m. On the main logging road and skid trails, $K_s$ values are similar to those found on unpaved logging roads in the Pacific Northwest, USA (see, e.g., Reid and Dunne, 1984; Luce and Cundy, 1994), where roads also tend to be deeply excavated into the hillslope profile (Table VI).

Through measurements of runoff on 22 m × 3 m plots at the Jengka Experimental Basin in Pahang, Peninsular Malaysia, Baharuddin *et al.* (1996) determined that annual ROCs for logging roads and skid trails ranged from 0·14 to 0·21 during a 2 year period (rainfall depths were 2310 and 3080 mm). In comparison, the aggregated ROC on the

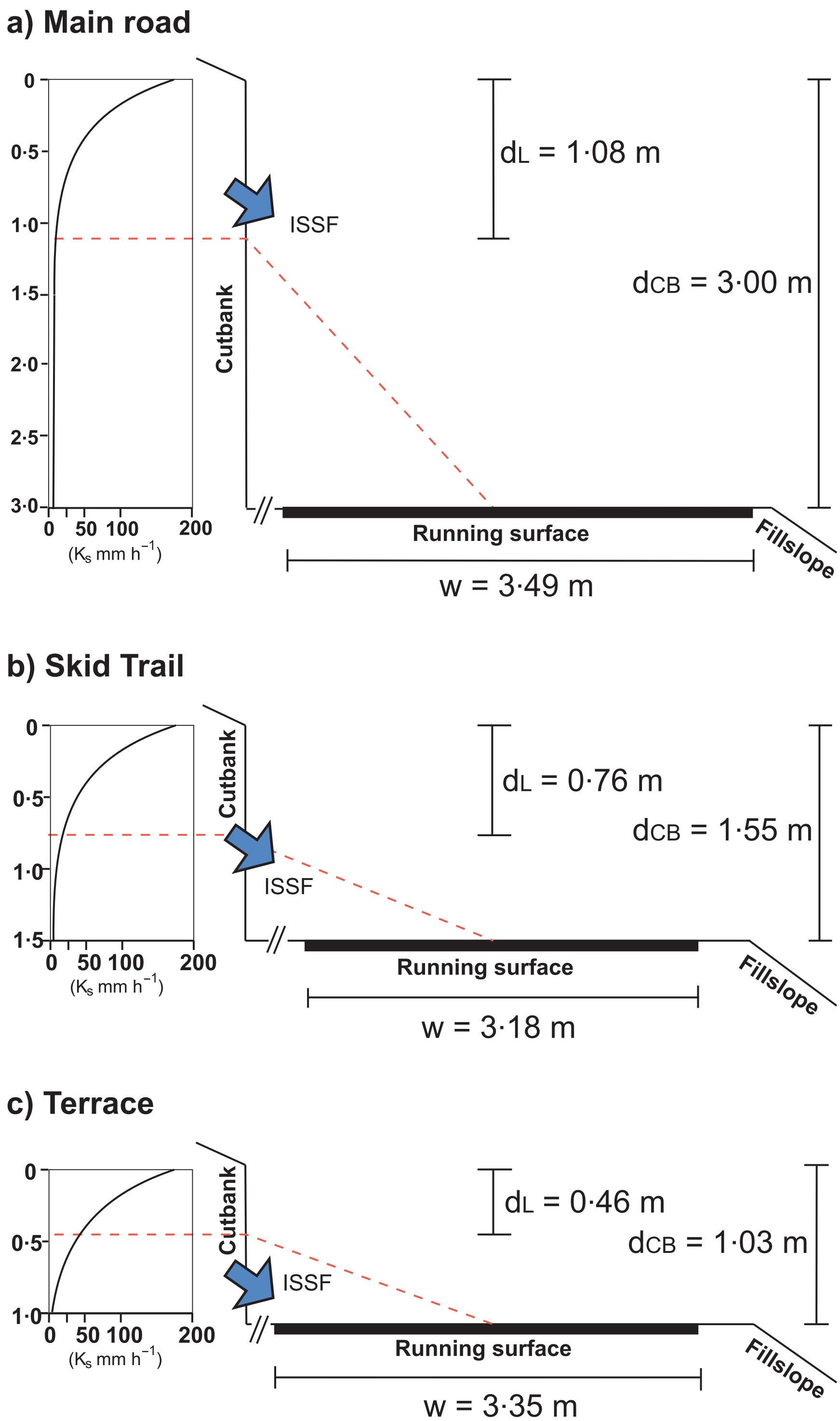


**Figure 8.** Median depth of the cutbank ($d_{CB}$), median surface lowering of the road surface ($d_L$) and median running surface width ($w$) for three types of road/trail in BTEC3. The dotted line indicates the depth in the adjacent soil profile that corresponds to the road surface; this line also identifies the corresponding value of depth-specific $K_s$. The thick arrow indicates the approximate depth at which intercepted subsurface flow (ISSF) was typically observed exfiltrating from the road cut on to the road surface. This figure is available in colour online at www.interscience.wiley.com/journal/espl



DOI: 10.1002/esp

main logging road in BTEC3 during 10 monitored storms was 0·53. The aggregated ROCs for the 17 simulated storms were even higher because of the abundance of large simulated events: terraces (0·79), skid trails (0·82) and the main logging road (0·86). If we assume that all 256 storms observed during our 2 year study follow the relationships shown in Figure 8, total ROCs (estimated via non-linear regression) range from 0·58 to 0·69 for the three types of BTEC road/trail. Collectively the simulations and the monitored storm data indicate runoff on BTEC roads was significantly higher than that found previously at Jengka. The Jengka roads, which were primarily paths/tracks used by lorries, were distinctly different from the BTEC3 main logging road and skid trails in terms of depth of excavation (Baharuddin *et al.*, 1996). As a result, $K_s$ on the Jengka roads was an order of magnitude higher than on these two types of BTEC road/trail: more than 20 versus 2 mm $h^{-1}$ or less (Baharuddin *et al.*, 1996; Table II).

## Limitations of the simulations

The modeled road section is represented in KINEROS2 as a singular planar element. Surface microtopography is incorporated via spacing and relief parameters; however, specific features that affect ponding and overland flow, such as rills and gullies, are not specifically included. In the real setting, the road area contributing to runoff varies during a given storm because of the spatial variation in infiltration and flow capture by rills/gullies. Variations in infiltrability are accounted for in KINEROS2 with the $C_vK_s$ parameter. The latter phenomenon is generalized via model calibration and testing, during which parameters were adjusted to minimize differences between simulated and observed hydrographs. Simulated flow is obviously not a perfect reproduction of on-road overland flow during all storms (as shown in Figure 6). Nevertheless, simulated flow is useful for estimating plausible differences in surface erosion and sediment delivery on each road type. However, the simulated values probably overestimate the total runoff to the stream system, because some unknown portion would undoubtedly re-infiltrate on hillslopes below areas where unconcentrated flow exists the road.

## Traffic impacts and compaction

Our first hypothesis was that the various road/trail types in BTEC3 would differ greatly in hydrological response because of differences in the extent of traffic. However, all types of road/trail produced substantial HOF during most simulated events (Figure 7). These patterns in HOF generation largely reflected the small observed differences in $K_s$: e.g. the low-$K_s$ main logging road generated the most HOF per unit area, and terraces, which had the highest near-surface $K_s$, the least. However, there was very little difference in simulated HOF between the main logging road and the skid trails because of the high intensity of the simulated rainfall events.

The reduction in simulated HOF on terraces, the roads undergoing the least traffic, was facilitated by storage of rainwater in the loose layer of side-cast material deposited on the surface (typically >0·10 m deep). However, consolidated subsoil and/or saprolite with naturally low $K_s$ existed immediately beneath this unconsolidated material, similar to the other road types. Once rainfall exceeded the storage capacity of the loose side-cast soil, HOF initiated. Nine months after the initial $K_s$ measurement campaign most of the loose surface material on the terraces had been removed by water erosion. Thus, the relatively high $K_s$ that was initially measured was not representative of near-surface $K_s$ on the terraces over longer time periods. Therefore, the simulated HOF values shown in Table VIII probably underestimate surface runoff generated on terraces.

The main logging road and skid trails were created with a bulldozer; the terraces were excavated with a backhoe. None of the roads were heavily compacted beyond that sustained during the excavation process, which mainly pushed fill material downslope. Subsequent traffic on wet road surfaces probably served more to displace and puddle loose soils, rather than facilitate additional compaction. Thus, the propensity for all three types of road in BTEC3 to generate HOF during most simulated storms was mainly related to the fact that they were excavated at least 0·5–1·0 m into the hillslope profile (cf. Malmer and Gripp, 1990). These depths coincide with weathered subsoil horizons, saprolite and/or bedrock – all of which have low saturated hydraulic conductivities (Table I; Ziegler *et al.*, 2006). The estimated 'lowering' values due to excavation were determined at the road centerline (Table III; Figure 8). The inside portion of the roads were even more deeply excavated into the hillslope regolith (e.g. 2–3 m on the main logging road).

## Influence of recovery time after abandonment on HOF generation

Our second hypothesis was that HOF generation would be rare on the abandoned skid trail in BTEC1 because substantial vegetation, including medium-sized trees, had emerged in the 40 years since abandonment. Unlike the other types of road, ground and canopy cover was significant (estimated at 80%). In addition, the road surface consisted of a thin (<5 cm), organic-rich soil layer with relatively high $K_s$ (median = 62 mm $h^{-1}$). However, $K_s$ was still



DOI: 10.1002/esp

significantly lower than that in the upper 10 cm of the adjacent non-roaded hillslope (675 mm $h^{-1}$, Table V). Despite vegetation regrowth, $K_s$ at 0·25 m was not significantly different from that for all the other types of road investigated (<6 mm $h^{-1}$; Table II). Similar to terraces in BTEC3, HOF was simulated frequently on the abandoned skid trail for events >25 mm (Figure 7). HOF was simulated for large storms because the permeable near-surface layer had a limited capacity to store infiltrated water. Although substantial recovery in vegetation had taken place in 40 years, the excavation of this road into the low-permeability regolith dictated the occurrence of HOF during large simulated events.

The hydrologic benefits of the 40 year recovery on the abandoned skid trail can be seen by comparing simulated HOF on the entire road/trail network in BTEC3 (main road, skid trails and terraces combined) with the scenario that all roads/trails have recovered to a condition that is similar to that of the abandoned skid trail (including canopy and ground cover). For the total applied rainfall (822 mm; 17 storms), simulated basin-wide HOF from all roads/trails declined by almost 50% from 5326 to 2729 $m^3$ (Table VIII). This reduction is slightly greater than the estimated reduction in road runoff caused by pioneering ferns invading the main logging road in BTEC3 (Negishi *et al.*, 2006).

The estimated reduction in basin-wide HOF represents a substantial volume of surface runoff that would ordinarily contribute to surface erosion and delivery of eroded material to the stream network (Sidle *et al.*, 2004). Vegetation recovery on the abandoned skid trail provides additional benefits related to runoff generation and sediment production by increasing surface roughness, thus reducing flow velocity and promoting temporary ponding of water on the disturbed surfaces (Morgan, 1995). Such beneficial effects are not captured by looking only at $K_s$ measurements and/or diagnostic HOF simulations. Additionally, the multi-tiered canopy of the regenerating forest should also reduce some of the raindrop energy that currently exacerbates splash erosion on the unprotected roads and hillslopes in BTEC3 (Sidle *et al.*, 2004).

## Long-term impacts

Investigating abandoned skid trails in Sg. Tekam Forest Reserve (Peninsular Malaysia), Kamaruzaman (1996) found that surface bulk density was elevated by 20% and $K_s$ decreased by 76%, compared with nearby undisturbed lands, even after 10 years. He estimated via linear regression that bulk density on a variety of logging-related roads/surfaces would recover to background values in about 20 years; roughly 50 years, however, would be needed for full recovery of $K_s$. If we also assume a linear recovery rate, the estimated time of recovery for bulk density on BTEC skid trails is 45 years (Figure 9). In contrast, little recovery in $K_s$ would occur in 100 years.

Similar to our findings in BTEC3 are those of Malmer and Gripp (1990), who measured bulk density and infiltrability on mechanized logging tracks at Sipitang (Sabah, Malaysia). There, bulldozers created tracks that were in some locations excavated 1 m into the hillslope profile, occasionally exposing saprolite. Surface (0–5 cm) bulk density on tracks constructed on clay soils increased from 0·82 to 1·28 Mg $m^{-3}$ following construction. In six years, bulk density recovered to 1·16 Mg $m^{-3}$. Infiltrability, which initially declined from 154 to 0·3 mm $h^{-1}$, recovered only slightly (1·3 mm $h^{-1}$). Based on this rate of recovery, several hundred years would be needed for a full recovery in $K_s$. Bulk density would, however, recover in about 20 years (Figure 9).

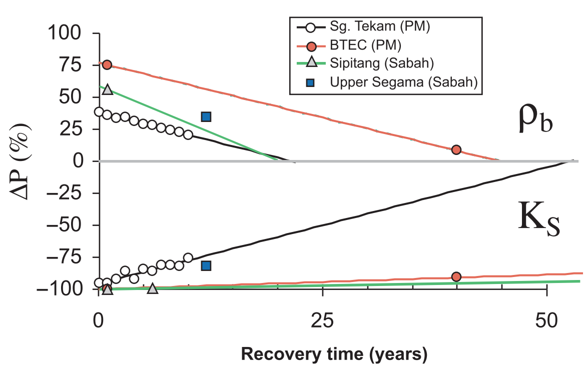


**Figure 9.** Percentage changes (Equation (3)) in bulk density ($\rho_b$) and saturated hydraulic conductivity ($K_s$), relative to undisturbed lands, are shown for abandoned skid trails at Sg. Tekam (Kamaruzaman, 1996), mechanized logging tracks at Sipitang (Malmer and Gripp, 1990), logging tracks in the Upper Segama (Van der Plas and Bruijnzeel, 1993), and the abandoned skid trail in BTEC1. The symbols represent measurements. The lines track the estimated recovery in the properly over time (via linear regression); full recovery occurs where lines cross the *x*-axis at zero. This figure is available in colour online at www.interscience.wiley.com/journal/espl

Collectively, these data suggest that when roads are excavated into consolidated hillslope regoliths, such as in BTEC and Sipitang, the concept of 'recovery' of $K_s$ has little practical meaning. Full recovery would require the development of a deep soil layer on the road surface. Even if aided by amelioration techniques (e.g. ripping), recovery would take longer than that for tracks impacted by surface compaction alone (cf. Kidd and Haupt, 1968; Luce, 1997; Reisinger *et al.*, 1992; Kolka and Smidt, 2004).

Again, overshadowing the concept of recovery of $K_s$ on the road surface (which would reduce HOF generation) is the influence of deep excavation on other runoff generation processes. For example, we commonly observed water exfiltrating onto roads from cutbanks via seeps occurring at the soil/saprolite interface and through fractured bedrock (ISSF, shown by the arrows in Figure 8). In addition, several road cuts had biogenic pipes that were activated during most storms (Negishi *et al.*, 2006, 2007). Although it is foreseeable that road $K_s$ could recover sufficiently over time to reduce HOF generation – as demonstrated to some degree by the abandoned skid trail in BTEC1 – a natural reduction in ISSF by deep road cuts is unlikely. For example, after 40 years the abandoned skid trail still actively intercepts subsurface flow.

While the persistence of HOF on 'revegetated' roads and trails may not cause excessive on-road erosion long after construction, hydrological impacts may still exist. For example, if the road affects the delivery of storm runoff to streams, there is a potential for the road network to enhance flood peaks, diminish low flows and destabilize hillslopes even after disturbed forest hillslopes have fully recovered. Furthermore, although sediment transport from roads/trails to the stream diminishes greatly within 2 years in BTEC3 (Sidle *et al.*, 2004, 2006), large events are capable of eroding the consolidated substrate material comprising road and skid trail surfaces because large volumes of runoff are generated on the extensive, connected road system (Figure 10).

## Impact reduction

Road removal, which may involve major re-contouring of the hillslope, has been applied elsewhere with the goal of reducing environmental impacts related to roads (Madej, 2001; Switalski *et al.*, 2004). The costs associated with these

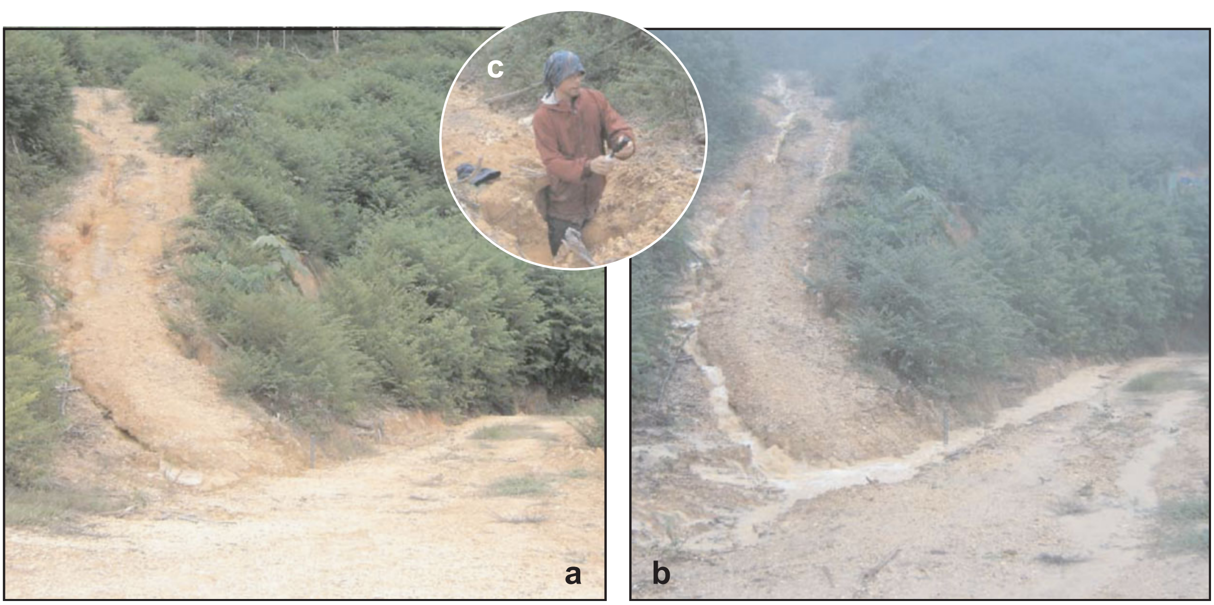


**Figure 10.** Severe erosion is exacerbated on this 66 m skid trail section by runon water from upslope skid trails. Surface flow on the skid trail itself is generated by the Horton mechanism. Another 255 m of upslope trails contribute additional flow from three sources: (1) Horton flow; (2) return flow from shallow pipes and (3) interception of subsurface flow by the cutbank. The runoff shown in panel b was during the 79 mm event No. 5 (5 November 2004), which had a maximum 10 min intensity of 102 mm $h^{-1}$ (Table III). Runoff water from upslope trails augments Hortonian overland flow generated on this road section, thereby increasing the total contributing hillslope area from about 260 $m^2$ of road surface to over 6000 $m^2$ of hillslope, including an additional 900 $m^2$ for HOF generation. The median width and depth of the gully is 0·37 and 0·23 m, and maximum depth exceeds 0·5 m (panel c). This equates to about 5·7 $m^3$, or 9·1 Mg of material, that was delivered to the stream system in only 8 months following logging. This figure is available in colour online at www.interscience.wiley.com/journal/espl



DOI: 10.1002/esp

types of activity are probably not justifiable for most logging sites in SE Asia, particularly for sites where road density is as high as in BTEC3. In addition, evidence is not yet available that demonstrates that these measures do indeed restore hillslope flow pathways or are economically viable in terms of landslide reduction (Allison *et al.*, 2004; Switalski *et al.*, 2004). Thus, the most cost-effective means to avoid adverse hydrological changes from logging road construction is by effective long-term planning of the road/skid trail system, including minimizing road/trail density, avoiding excessive excavation on midslope sites, minimizing steep skid trails draining directly into forest roads, avoiding wet and unstable sites (e.g. geomorphic hollows), and determining the ultimate lifetime of the road/trail system (see, e.g., Sidle, 1980; Megahan, 1987; Baharuddin, 1995; Allison *et al.*, 2004; Sidle and Ochiai, 2006). This is particularly important in locations where substantial subsurface flow is intercepted by the road prism and/or a high percentage of the total rainfall comes from intense rain storms, as is the case in BTEC.

## Final considerations

The reported findings are preliminary. Some of the differences in the near-surface versus 0·25 m $K_s$ measurements could be related to the different methods employed. For example, the surface $K_s$ values on the abandoned skid trail were lower than one might anticipate for a revegetated surface. However, all $K_s$ values were in line with those reported for various types of road in studies conducted elsewhere. Our field data show a much slower rate of recovery in $K_s$ than for bulk density compared to other studies in Malaysia, suggesting that bulk density itself is not a reliable index for assessing the recovery of soil hydrological properties following logging. We also recognize that point measurements of $K_s$ often do not represent the hillslope-scale permeability that controls hydrological response (cf. Croke *et al.*, 2001). This may be particularly true for the abandoned skid trail. We incorporated the diagnostic HOF simulations, in part, to account for the limitations in the direct interpretation of point measurements of $K_s$.

Furthermore, the HOF simulations were particularly helpful in exploring the influence of variable $K_s$ with depth on HOF generation from roads/trails. These simulations provide more insight than simply comparing $K_s$ among road types. In particular, they highlighted the importance of a flow-restricting subsurface layer on the generation of HOF from road surfaces with thin surface soils of high infiltrability, but limited water storage capacity. While the relative differences in simulated HOF generation are consistent with observations, explicit interpretation of the absolute values is not recommended because (i) we had limited validation data at the hillslope-scale for all road types and (ii) the simulations were performed for one initial soil moisture state. Additional work in BTEC3 should address quantifying road runoff on monitored road sections for a variety of field conditions and road types.

# Conclusion

All types of logging road/trail investigated, regardless of design and usage, partitioned substantial percentages of rainfall into HOF during nearly all storms, primarily because they were excavated into hillslope material of low $K_s$. Even a skid trail that was abandoned for 40 years and had substantial vegetation regrowth generated HOF for storms above 25 mm because the recovery in $K_s$ only occurred within the upper few centimeters of the road surface. Little recovery in surface $K_s$ was estimated to occur on roads within a time span of 100–200 years. Excavation of roads into the hillslope regolith further contributed to road-related overland flow generation through the interception of subsurface flow and return flow emerging from shallow biogenic pipes. Recovery of pre-road hydrological response is exceptionally slow because the only phenomena that promote deep infiltration of rain water are covering of the road surface with soil (either by rehabilitation or mass wasting) or the development of new soil via weathering, which includes the effects of colonizing vegetation. Natural recovery or rehabilitation techniques that simply hasten the emergence of vegetation on abandoned skid trails may reduce the propensity to generate HOF; however, subsurface flow would still likely be intercepted by the cutbank, thereby contributing to the persistence of hydro-geomorphological impacts of roads indefinitely. Thus, the key to reducing the long-term impacts associated with logging roads at sites such as BTEC is efficient road network planning, which includes minimizing total road length – especially if roads are excised deeply into the hillslope profile.

## Acknowledgements

Funding for this field research was provided by the National University Singapore grant R-109-000-031-112 to Roy Sidle, in collaboration with Forest Research Institute Malaysia (FRIM) and Japan International Research Center for Agricultural Sciences (JIRCAS). Junjiro Negishi was supported by a National University Singapore (NUS) Graduate Fellowship and Singapore Millennium Scholarship. Support for Alan Ziegler was provided by NUS, JIRCAS and a Japan Society for the Promotion of Science (JSPS) fellowship. Roy Sidle was partly supported by a JSPS research grant. We also thank Mahmoud and Linda for their assistance.

## References

Allison C, Sidle RC, Tait D. 2004. Application of decision analysis forest road deactivation in unstable terrain. *Environmental Management* **33**: 173–185.

Amoozegar A. 1989. Comparison of the Glover solution with the simultaneous equations approach for measuring hydraulic conductivity. *Soil Science Society of America Journal* **53**: 1362–1367.

Amoozegar A. 1992. Compact constant head permeameter: a convenient device for measuring hydraulic conductivity. In *Advances in Measurement of Soil Physical Properties: Bringing Theory Into Practice*, Special Publication 30, Topp CG (ed.). Soil Science Society of America: Madison, WI; 31–42.

Amoozegar A, Warrick W. 1986. Hydraulic conductivity of saturated soils: field methods. In *Methods of Soil Analysis, Part 1. Physical and Mineralogical Methods*, Agronomy Monograph 9, 2nd edn, Klute A (ed.). ASA–CSSA–SSSA: Madison, WI; 735–770.

Baharuddin K. 1988. Effects of logging operations on physical properties and soil erosion in a hill dipterocarp forest of Peninsular Malaysia. *Journal of Tropical Forest Science* **1**: 56–66.

Baharuddin K. 1995. *Effects of Logging Operations on Physical Properties and Soil Erosion in a Hill Dipterocarp Forest of Peninsular Malaysia*, Research Pamphlet 119. Forest Research Institute Malaysia: Kuala Lumpur.

Baharuddin K, Abdul Rahim N. 1994. Suspended sediment yield resulting from selective logging practices in a small watershed in Peninsular Malaysia. *Journal of Tropical Forest Science* **7**: 286–295.

Baharuddin K, Mokhtaruddin AM, Majid NM. 1996. Effects of logging on soil physical properties in Peninsular Malaysia. *Land Husbandry* **1**: 33–41.

Beschta RL. 1978. Long-term patterns of sediment production following road construction and logging in the Oregon Coast Range. *Water Resources Research* **14**: 1011–1016.

Bren LJ, Leitch CJ. 1985. Hydrologic effects of a stretch of forest road. *Australian Forestry Research* **15**: 183–194.

Brooks SM, Richards KS, Nussbaum R. 1994. Simulator experiments of the varied consequences of rain forest logging for runoff and erosion. *Geografiska Annaler, Series A, Physical Geography* **76**: 143–152.

Brooks SM, Spencer T. 1997. Changing soil hydrology due to rain forest logging: an example from Sabah Malaysia. *Journal of Environmental Management* **49**: 297–310.

Bruijnzeel LA. 1990. *Hydrology of Moist Tropical Forest and Effects of Conversion: a State of Knowledge Review*. UNESCO: Paris–Vrije Universiteit: Amsterdam.

Burroughs ER Jr., Marsden MA, Haupt HF. 1972. Volume of snowmelt intercepted by logging roads. *Journal of Irrigation and Drainage Division ASCE* **98**: 1–12.

Cederholm CJ, Reid LM, Salo EO. 1981. Cumulative effects of logging road sediment on salmonoid populations in the Clearwater River, Jefferson County, Washington. In *Salmon-Spawning Gravel, a Renewable Resource in the Pacific Northwest*, Paper 39. Washington Water Research Center: Pullman, WA; 38–74.

Chappell NA, Douglas I, Hanapi JM, Tych W. 2004. Sources of suspended sediment within a tropical catchment recovering from selective logging. *Hydrological Processes* **18**: 685–701.

Chappell NA, Ternan JL. 1997. Ring permeametry: design, operation, and error analysis. *Earth Surface Processes and Landforms* **22**: 1197–1205.

Commandeur PR, Wass EF. 1994. *Rainfall Simulation, Soil Infiltration, and Surface Erosion on Skidroad Surfaces – Nelson Forest Region*. B.C. Ministry of Forestry: Victoria, B.C., Canada.

Croke J, Hairsine P, Fogarty P. 2001. Soil recovery from track construction and harvesting changes in surface infiltration, erosion and delivery rates with time. *Forest Ecology and Management* **143**: 3–12.

Croke J, Mockler S, Harisine P, Fogarty P. 2006. Relative contributions of runoff and sediment from sources within a road prism and implications for total sediment delivery. *Earth Surface Processes and Landforms* **31**: 457–468.

Dickerson BP. 1976. Soil compaction after tree-length skidding in northern Mississippi. *Soil Science Society of America Journal* **40**: 965–966.

Douglas I, Bidin K, Balamurugan G, Chappell NA, Walsh RPD, Greer T, Sinum W. 1999. The role of extreme events in the impacts of selective harvesting and recovery phases at Danum Valley, Sabah. *Philosophical Transactions of the Royal Society of London B* **354**: 1749–1761.

Fahey BD, Coker RJ. 1992. Sediment production from forest roads in Queen Charlotte Forest and potential impact on water quality, Marlborough Sounds, New Zealand. *New Zealand Journal of Marine and Freshwater Research* **26**: 187–195.

Forman RTT, Alexander LE. 1998. Roads and their major ecological effects. *Annual Review of Ecology and Systematics* **29**: 207–231.

Froehlich HA. 1979. Soil compaction from logging equipment: effects on growth of young ponderosa pine. *Journal of Soil and Water Conservation* Nov/Dec: 276–278.

Garder BD, Chong SK. 1990. Hydrologic responses of compacted forest soils. *Journal of Hydrology* **112**: 327–334.

Gomi T, Sidle RC, Noguchi S, Negishi JN, Abdul Rahim N, Sasaki S. 2006. Sediment and wood accumulations in humid tropical headwater streams: effects of logging and riparian buffers. *Forest Ecology and Management* **224**: 166–176.

Grayson RB, Haydon SR, Jayasuriya MDA, Finlayson BL. 1993. Water quality in mountain ash forests – separating the impacts of roads from those of logging operations. *Journal of Hydrology* **150**: 459–480.

Greacen EL, Sands R. 1980. A review of compaction of forest soils. *Australian Journal of Soil Research* **18**: 163–189.

Gucinski H, Furniss MJ, Ziemer RR, Brookes MH (eds). 2000. *Forest Roads: a Synthesis of Scientific Information*, General Technical Report PNW-GTR-509. USDA Forest Service: Portland, OR.



DOI: 10.1002/esp

Guillemette F, Plamondon AP, Prevost M, Levesque D. 2005. Rainfall generated stormflow response to clearcutting a boreal forest: peak flow comparison with 50 world-wide basin studies. *Journal of Hydrology* **302**: 137–153.

Hafley WL. 1975. Rural road systems as a source of sediment pollution – a case study. In *Watershed Management: Symposium Conducted by the Committee on Watershed Management of the Irrigation and Drainage Division of the American Society of Civil Engineers Utah Section, ASCE*, Logan, UT, 1975. American Society of Civil Engineers, Committee of Watershed Management: New York; 393–405.

Harr RD, Harper WC, Krygier JT, Hsieh FS. 1975. Changes in storm hydrographs after road building and clear-cutting in the Oregon Coast Range. *Water Resources Research* **11**: 436–444.

Hatchell GE, Ralston CW, Foil RR. 1970. Soil disturbances in logging: effects on soil characteristics and growth of loblolly pine in the Atlantic Coastal Plane. *Journal of Forestry* Dec: 772–775.

Hillel D. 1971. *Soil and Water – Physical Principles and Processes*. Academic: New York.

Incerti M, Clinnick PF, Willatt ST. 1987. Changes in the physical properties of a forest soil following logging. *Australian Forest Research* **13**: 305–308.

Jakobsen BF. 1983. Persistence of compaction effects in a forest Raznozem. *Australian Forest Research* **13**: 305–308.

Johnson MG, Beschta RL. 1980. Logging, infiltration capacity and surface erodibility in western Oregon. *Journal of Forestry* **78**: 334–337.

Jones JA. 2000. Hydrologic processes and peak discharge response to forest removal, regrowth, and roads in 10 small experimental basins, western Cascades, Oregon. *Water Resources Research* **36**: 2621–2642.

Jones JA, Swanson FJ, Wemple BC, Snyder KU. 2000. Effects of roads on hydrology, geomorphology, and disturbance patches in stream networks. *Conservation Biology* **14**: 76–85.

Kamaruzaman J. 1996. Estimation of rate of recovery of disturbed soils from ground-based logging in peninsular Malaysia. *Journal of Tropical Forest Science* **9**: 88–100.

Keppeler ET, Ziemer RR. 1990. Logging effects on streamflow: water yield and summer low flows at Caspar Creek in Northwest California. *Water Resources Research* **26**: 1669–1679.

Kidd WJ, Haupt HF. 1968. *Effects of Seedbed Treatment on Grass Establishment on Logging Roadbeds in Central Idaho*, Research Paper INT-53. USDA, Forest Service, IRS: Ogden, UT.

King JG, Tennyson LC, 1984. Alteration of streamflow characteristics following road construction in north central Idaho. *Water Resources Research* **20**: 1159–1163.

Kolka RK, Smidt MF. 2004. Effects of forest road amelioration techniques on soil bulk density, surface runoff, sediment transport, soil moisture and seedling growth. *Forest Ecology and Management* **202**: 313–323.

La Marche JL, Lettenmaier DP. 2001. Effects of forest roads on flood flows in the Deshutes River, Washington. *Earth Surface Processes and Landforms* **26**: 115–134.

Lane PHJ, Sheridan GJ. 2002. Impact of an unsealed forest road stream crossing: water quality and sediment sources. *Hydrological Processes* **16**: 2599–2612.

Loague K, Gander GA. 1990. R-5 revisited: 1. Spatial variability of infiltration on a small rangeland catchment. *Water Resources Research* **26**: 957–971.

Luce CH. 1997. Effectiveness of road ripping in restoring infiltration capacity of forest roads. *Restoration Ecology* **5**: 265–270.

Luce CH. 2002. Hydrological processes and pathways affected by forest roads: what do we still need to learn? *Hydrological Processes* **16**: 2901–2904.

Luce CH, Black TA. 1999. Sediment production from forest roads in western Oregon. *Water Resources Research* **35**: 2561–2570.

Luce CH, Cundy TW. 1994. Parameter identification for a runoff model for forest roads. *Water Resources Research* **30**: 1057–1069.

MacDonald LH, Sampson RW, Anderson DM. 2001. Runoff and road erosion at the plot and road segment scales, St. John, US Virgin Islands. *Earth Surface Processes and Landforms* **26**: 251–272.

Madej M. 2001. Erosion and sediment delivery following removal of forest roads. *Earth Surface Processes and Landforms* **26**: 175–190.

Malmer A. 1996. Hydrological effects and nutrient losses of forest plantation establishment on tropical rainforest land in Sabah, Malaysia. *Journal of Hydrology* **174**: 129–148.

Malmer A, Grip H. 1990. Soil disturbance and loss of infiltrability caused by mechanized and manual extraction of tropical rainforest in Sabah, Malaysia. *Forest Ecology and Management* **38**: 1–12.

Megahan WF. 1972. Subsurface flow interception by a logging road in mountains of central Idaho. In *Proceedings, National Symposium on Watersheds in Transition*. American Water Resources Association: Fort Collins, CO; 350–356.

Megahan WF. 1974. *Erosion over Time: a Model*, USDA-Forest Service Research Paper Report INT-156. Intermountain Research Station: Ogden, UT.

Megahan WF. 1983. Hydrologic effects of clearcutting and wildfire on steep granitic slopes in Idaho. *Water Resources Research* **19**: 811–819.

Megahan WF. 1987. Effects of forest roads on watershed function in mountainous areas. In *Environmental Geotechnics and Problematic Soils and Rocks*, Balasubramaniam AS, Chandra S, Bergado DT, Nutalaya P (eds). Balkema: Rotterdam; 335–348.

Megahan WF. 1988. Roads and forest site productivity. In *Degradation of Forested Land: Forest Soils at Risk; Proceedings of the 10th B.C. Soil Science Workshop*, 1986, Lousier JD, Stills DW (eds). British Columbia Ministry of Forestry: Victoria, BC, Canada; 54–65.

Montgomery DR. 1994. Road surface drainage, channel initiation, and slope instability. *Water Resources Research* **30**: 1925–1932.

Morgan RPC. 1995. *Soil Erosion and Conservation*. Longman: Essex, UK.

Nash JE, Sutcliffe JV. 1970. River flow forecasting through conceptual models, 1, a discussion of principles. *Journal of Hydrology* **10**: 282–290.

Negishi JN. 2005. *Understanding Intra-Catchment Processes Related to Management of Tropical Headwater Catchments*, Ph.D. dissertation, National University of Singapore.

Negishi JN, Noguchi S, Sidle RC, Ziegler AD, Abdul Rahim N. 2007. Stormflow generation involving soil pipes in a tropical zero-order basin of Peninsular Malaysia. *Hydrological Processes* in press.

Negishi JN, Sidle RC, Noguchi S, Abdul Rahim N, Stanforth R. 2006. Ecological roles of roadside fern (Dicranopteris curranii) on logging road recovery in Peninsular Malaysia: preliminary results. *Forest Ecology and Management* **224**: 176–175.

Noguchi S, Abdul Rahim N, Baharuddin K, Sammori T, Tani M, Tsuboyama Y. 1996. Rainfall characteristics of tropical rain forest and temperate forest: comparison between Bukit Tarek in Peninsular Malaysia and Hitachi Ohta in Japan. *Journal of Tropical Forest Science* **9**: 206–220.

Noguchi S, Abdul Rahim N, Shamsuddin SA, Shahar A. 2005. Spatial variability of throughfall along old logging road in Bukit Tarek Experimental Watershed. In: *Rehabilitation of Degraded Tropical Forests, Southeast Asia 2005*, proceedings of the International Workshop on the Landscape Level Rehabilitation of Degraded Tropical Forest, 2005. LLRDTFR Project: Tsukuba, Japan.

Parlange J-Y, Lisle I, Braddock RD, Smith RE. 1982. The three-parameter infiltration equation. *Soil Science* **133**: 337–341.

Perry TO. 1964. Soil compaction and loblolly pine growth. *USFS Tree Planters' Notes* **67**: 9.

Philip JR. 1957. The theory of infiltration: 1. The infiltration equation and its solution. *Soil Science* **83**: 345–357.

Phillips C. 1986. Preliminary observation on the effects of logging on the hill forest in Sabah. In *Proceedings of Workshop on Impact of Man's Activities on Tropical Upland Forest Ecosystems*, Yusof H, Kamis A, Nik MM, Shukri M (eds). University of Agriculture Malaysia: Serdang, Selangor, Malaysia; 187–215.

Pinard MA, Barker MG, Tay J. 2000. Soil disturbance and post-logging forest recovery on bulldozer paths in Sabah, Malaysia. *Forest Ecology and Management* **130**: 213–225.

Rab MA. 1996. Soil physical and hydrological properties following logging and slash burning in the *Eucalyptus regnans* forest of Southeastern Australia. *Forest Ecology and Management* **84**: 159–176.

Rab MA. 2004. Recovery of soil physical properties from compaction and soil profile disturbance caused by logging of native forest in Victorian Central Highlands, Australia. *Forest Ecology and Management* **191**: 329–340.

Rawls WJ, Brakensiek DL, Saxton KE. 1982. Estimation of soil water properties. *Transactions of the American Society of Agricultural Engineers* **2**(5): 1316–1320, 1328.

Reid LM, Dunne T. 1984. Sediment production from forest road surfaces. *Water Resources Research* **20**: 1753–1761.

Reinhart KG. 1964. Effect of a commercial clearcutting in West Virginia on overland flow and storm runoff. *Journal of Forestry* **62**: 167–171.

Reisinger TW, Pope PW, Hammond SD. 1992. Natural recovery of compacted soils in an upland hardwood forest in Indiana. *Northern Journal of Applied Forestry* **9**: 138–141.

Riley SJ. 1984. Effect of clearing and roading operation on the permeability of forest soils, Karuah Catchment, New South Wales, Australia. *Forest Ecology and Management* **9**: 283–293.

Roe FW. 1951. *The Geology and Mineral Resources of the Fraser's Hill Area Selangor, Perek, and Pahang, Federation of Malaya with an Account of the Mineral Resources*. Caxton: Kuala Lumpur.

Saifuddin S, Abdul Rahim N, Abdul Rashid MF. 1991. *Watershed Research in Forest Plantation: 1. Establishment and Physical Characteristics of Bukit Tarek Watershed*, Research Pamphlet 110. Forest Research Institute Malaysia: Kuala Lumpur.

Sidle RC. 1980. *Impacts of Forest Practices on Surface Erosion*, Pacific Northwest Extension Publication PNW-195. Oregon State University: Corvallis, OR.

Sidle RC, Ochiai H. 2006. *Landslides: Processes, Prediction, and Land Use*, American Geophysical Union (AGU) Water Resources Monograph 18. AGU: Washington, DC.

Sidle RC, Sasaki S, Otsuki M, Noguchi S, Abdul Rahim N. 2004. Sediment pathways in a tropical forest: effects of logging roads and skid trails. *Hydrological Processes* **18**: 703–720.

Sidle RC, Ziegler AD, Negishi JN, Abdul Rahim N, Siew R, Turkelboom F. 2006. Erosion processes in steep terrain – truths, myths, and uncertainties related to forest management in Southeast Asia. *Forest Ecology and Management* **224**: 199–225.

Smith RE, Goodrich DC, Quinton JN. 1995. Dynamic, distributed simulation of watershed erosion: the KINEROS2 and EUROSEM models. *Journal of Soil Water Conservation* **50**: 517–520.

Smith RE, Goodrich DC, Unkrich CL. 1999. Simulation of selected events on the Catsop catchment by KINEROS2: a report for the GCTE conference on catchment scale erosion models. *Catena* **37**: 457–475.

Smith RE, Smettem KRJ, Broadbridge P, Woolhiser DA. 2002. *Infiltration Theory for Hydrologic Applications*. American Geophysical Union: Washington, DC.

Storck P, Bowling L, Wetherbee P, Lettenmaier D. 1997. Application of a GIS-based distributed hydrology model for prediction of forest harvest effects on peak stream flow in the Pacific Northwest. *Hydrological Processes* **12**: 889–904.

Sutherland RA, Bussen JO, Plondke DL, Evans BL, Ziegler AD. 2001. Hydrophysical degradation associated with hiking trail use: a case study of Hawai'iloa Ridge Trail, Oahu, Hawai'i. *Land Degradation and Development* **12**: 71–86.

Swift LW Jr. 1984. Gravel and grass surfacing reduces soil loss from mountain roads. *Forest Science* **30**: 657–670.

Switalski TA, Bissonette JA, DeLuca TH, Luce CH, Madej MA. 2004. Benefits and impacts of road removal. *Frontiers in Ecology and the Environment* **2**: 21–28.

Thomas RB, Megahan WF. 1998. Peak flow responses to clear-cutting and roads in small and large basins, western Cascades, Oregon: a second opinion. *Water Resources Research* **34**: 3393–3403.

Van der Plas MC, Bruijnzeel LA. 1993. Impact of mechanized selective logging of rainforest on topsoil infiltrability in the Upper Segama areas, Sabah, Malaysia. *IAHS* **216**: 203–211.

Webb RH. 2002. Recovery of severely compacted soils in the Mojave Desert, California, USA. *Arid Land Research and Management* **16**: 291–305.




DOI: 10.1002/esp

Wemple BC, Jones JA, Grant GE. 1996. Channel network extension by logging roads in two basins, Western Cascades, Oregon. *Water Resources Bulletin* **32**: 1195–1207.

Wemple BC, Swanson FJ, Jones JA. 2001. Forest roads and geomorphic interactions, Cascade Range, Oregon. *Earth Surface Processes and Landforms* **26**: 191–204.

White I, Sully MJ. 1987. Macroscopic and microscopic capillary length and time scales from field infiltration. *Water Resources Research* **23**: 1514–1522.

Woolhiser DA, Smith RE, Goodrich DA. 1990. *KINEROS, a Kinematic Runoff and Erosion Model: Documentation and User Manual*, ARS-77. USDA-Agricultural Research Service.

Wright KA, Sendek KH, Rice RM, Thomas RB. 1990. Logging effects on streamflow: storm runoff at Caspar Creek in Northwestern California. *Water Resources Research* **26**: 1657–1667.

Wyatt-Smith J. 1963. *Manual of Malayan Silviculture for Inland Forests*, Malaysian Forest Records 23.

Ziegler AD, Giambelluca TW. 1997. Importance of rural roads as source areas for runoff in mountainous areas of northern Thailand. *Journal of Hydrology* **196**: 204–229.

Ziegler AD, Giambelluca TW, Sutherland RA, Nullet MA, Yarnasarn S, Pinthong J, Preechapanya P, Jaiarree S. 2004. Toward understanding the cumulative impacts of roads in agricultural watersheds of Montane Mainland Southeast Asia. *Agriculture Ecosystems and Environment* **104**: 145–158.

Ziegler AD, Negishi JN, Sidle RC, Noguchi S, Abdul Rahim N. 2006. Impacts of logging disturbance on saturated hydraulic conductivity in a tropical forest in Peninsular Malaysia. *Catena* **67**: 89–102.

Ziegler AD, Sutherland RA. 2006. Effectiveness of a coral surfacing material in reducing sediment production on unpaved roads, Schoffield Barracks, Oahu, Hawaii. *Environmental Management* **37**: 98–110.

Ziegler AD, Sutherland RA, Giambelluca TW. 2000. Partitioning total erosion on unpaved roads into splash and hydraulic components: the roles of inter-storm surface preparation and dynamic erodibility. *Water Resources Research* **36**: 2787–2791.

Ziemer RR. 1981. Storm flow response to road building and partial cutting in small streams of northern California. *Water Resources Research* **17**: 907–917.

Zulkifli Y, Abdul Rahim N, Baharuddin K. 2000. Stream chemistry on rainforest catchments on metamorphic rock. *Proceedings, XXI International Union of Forestry Research Organizations (IUFRO) World Congress*, Kuala Lumpur, 2000.

Zulkifli Y, Anhar S. 1994. Effects of selective logging methods on suspended solids concentration and turbidity level in streamwater. *Journal of Tropical Forest Science* **14**: 213–222.



DOI: 10.1002/esp